

Mediterranean Marine Science

Vol 22, No 1 (2021)

Vol 22, No 1 (2021)



Spatio-temporal distribution of pufferfish (Tetraodontidae) along the Turkish coast of the Mediterranean Sea

ERHAN MUTLU, ILARIA DE MEO, CLAUDIA MIGLIETTA

doi: [10.12681/mms.23481](https://doi.org/10.12681/mms.23481)

To cite this article:

MUTLU, E., DE MEO, I., & MIGLIETTA, C. (2021). Spatio-temporal distribution of pufferfish (Tetraodontidae) along the Turkish coast of the Mediterranean Sea. *Mediterranean Marine Science*, 22(1), 1-19. <https://doi.org/10.12681/mms.23481>

Spatio-temporal distribution of pufferfish (Tetraodontidae) along the Turkish coast of the Mediterranean Sea

Erhan MUTLU¹, Ilaria de MEO² and Claudia MIGLIETTA³

¹ Akdeniz University, Fisheries Faculty, Main Campus, Antalya, Turkey

² Inland Norway University of Applied Sciences, Faculty of Applied Ecology, Agricultural Sciences and Biotechnology, Campus Evenstad, Elverum, Norway

³ Alimatha Island, Vaavu Atoll, Maldives

Corresponding author: emutlu@akdeniz.edu.tr

Contributing Editor: Murat BILECENOGLU

Received: 18 June 2020; Accepted: 12 October 2020; Published online: 8 January 2021

Abstract

Pufferfish represent a serious threat to the marine ecosystem in the Mediterranean Sea. To better understand the population dynamics of pufferfish and their relation with ecological parameters, six pufferfish species were studied in two fishing and one non-fishing zone in one of the most oligotrophic regions of the Mediterranean Sea during 2014 and 2015, including different habitats of vegetated and non-vegetated and seasons. The results provide information on pufferfish ecological status compared with more eutrophic zones in which these species could potentially worsen their impact. Four species were common in the study area and two were rare. The dominant species was *Lagocephalus suezensis*, reaching abundances of 11,000 ind/km² at 25 m in October, followed by *Lagocephalus sceleratus*, *Lagocephalus guentheri*, and *Torquigener flavimaculosus*. The rarest species, *Tylerius spinosissimus* and *Sphoeroides pachygaster*, reached higher abundance and biomass in October and February than the other sampling months. The riverine and meadow habitats played a crucial role for nursing and reproduction in the population dynamics of *Lagocephalus* species, while *T. flavimaculosus* was absent in these areas. Sex ratios changed depending on season and location. The occurrence of larger individuals of *Lagocephalus* spp. and *T. flavimaculosus* at greater depths evidenced an ontogenetic migration. Overall, length-weight (L-W) relationships indicate isometric growth for each of the species studied. Pufferfish populations were primarily a function of habitat and depth of seafloor and secondarily with water productivity.

Keywords: Pufferfish; distribution; density; biometry; Levantine Sea.

Introduction

Pufferfish are among the most invasive species in the marine environment, threatening ecosystems and posing health risks to humans and animals due to its production of tetrodotoxin (Streftaris & Zenetos, 2006; Beköz *et al.*, 2013; Belmaker *et al.*, 2013; Santhanam, 2018; Tamele *et al.*, 2019). Populations of pufferfish invaded the eastern Mediterranean Sea from the Indo-Pacific. Over time, the invasive pufferfish species experienced succession (Reina-Hervas *et al.*, 2004; Akyol *et al.*, 2005) and expansion towards eutrophic waters in the western Mediterranean Sea (Bedini 1998; Giordano *et al.*, 2012; Lipej *et al.*, 2013; Kara *et al.*, 2015; Deidun *et al.*, 2015; Azzurro *et al.*, 2016; Kleitou *et al.*, 2019). Only a few limited studies have been conducted in the oligotrophic eastern Mediterranean Sea (Ben-Abdallah *et al.*, 2011; Dulčić & Dragičević, 2014; Carbonara *et al.*, 2017; Al-Mabruk *et al.*, 2018; Kiparissis *et al.*, 2018).

Expansion of pufferfish species [i.e. *Lagocephalus sceleratus* (Gmelin, 1789)] have had negative impacts on the marine ecosystem (Kalogirou, 2013), fishery industry (Nader *et al.*, 2012; Ünal *et al.*, 2015; Öndes *et al.*, 2018), human health (Kan *et al.*, 1987; Yang *et al.*, 1996; Beköz *et al.*, 2013), and socioeconomic aspects of life in Turkey (Öndes *et al.*, 2018). The silver-cheeked toadfish *L. sceleratus* alone caused a loss of two million Euros in the Turkish fishing industry in one year (Ünal *et al.*, 2015).

The Black Sea and the eastern Mediterranean Sea are prime examples of the negative impact that invasive species can have on marine ecosystems (Kideys, 2002; Nader *et al.*, 2012; Kalogirou, 2013). Population dynamics of migrant species of pufferfish and their impact on marine ecosystems have not been extensively studied in their original localities or in other seas where pufferfish are less valued by commercial markets (Simon & Mazlan, 2008; Patmavathi *et al.*, 2017). Such migrant species can colonize rapidly after succession, limited only

by the abundance of nutrients, until an apex predator appears (Belmaker *et al.*, 2013). Three or four years ago, the lionfish *Pterois miles* (Bennett, 1828), which feed on juveniles and larvae of pufferfish, were invaded in the Mediterranean Sea and spread along the eastern coast of Turkey from east to west, increasing in fish size with time since its establishment (personal observation by Erhan Mutlu and Yaşar Özvarol along the Turkish coast of the Mediterranean, December 2018-January 2019 and June-July 2019).

Ten pufferfish spp. have been recorded in the Mediterranean Sea (Farrag *et al.*, 2016). In the eastern Mediterranean, particularly the Levantine Sea, pufferfish have been reported as single individuals (Corsini *et al.*, 2005; Corsini-Foka *et al.*, 2006, 2010; Fricke *et al.*, 2016; Alshawy *et al.*, 2019). Of the 10 pufferfish identified, 8 species were found along the Turkish coast (Turan *et al.*, 2017). Öndes *et al.* (2018) listed 7 species, but *Lagocephalus spadiceus* (Richardson, 1845) was believed to be missing and counted as a misidentified species in the eastern Mediterranean Sea. The misidentified *L. spadiceus* was replaced with *Lagocephalus guentheri* Miranda Ribeiro, 1915 (Matsuura *et al.*, 2011; CIESM, 2020).

Early studies on pufferfish focused mainly on initial reports on their first records (Bilecenoglu *et al.*, 2006; Tuncer *et al.*, 2008; Koç *et al.*, 2011; Turan & Yağlıoğlu, 2011; Irmak & Altınağaç, 2015; Akyol & Aydın, 2016, 2017; Çelik *et al.*, 2018), length-weight relationships (Başusta *et al.*, 2013a,b; Bilge *et al.*, 2017), population growth (Aydın, 2011; Farrag *et al.*, 2015), and biological parameters (Boustany *et al.*, 2015) of a single species when studying the spatio-temporal distribution of the pufferfish (Kalogirou, 2013; Farrag *et al.*, 2015; El-Haweet *et al.*, 2016; Özbek *et al.*, 2017).

Kalogirou *et al.* (2010, 2012) studied relationships between *Posidonia* spp. and fish assemblages, including two pufferfish identified as *L. sceleratus* as a seagrass resident and small individuals (15 cm) of *Lagocephalus suezensis* Clark & Gohar, 1953 as occasional visitors to the seagrass “meadow”. However, there are insufficient

ecological studies of pufferfish spp. in the Mediterranean to describe their population dynamics and environmental preferences by species and across time and space. Thus, the aim of this study was to investigate the distribution and population dynamics of pufferfish along the Turkish coast of the eastern Mediterranean Sea by analyzing data on density, size, and composition by sex of six pufferfish species found in different habitats, sub-regions, and bottom depths in the study area.

Materials and Methods

To study the distribution of pufferfish species in relation to environmental parameters, samples were seasonally collected with an otter trawl during different seasons over a period of two years (May 2014 and August 2014, October 2014 and February 2015). The otter trawl was made of polyethylene with a head-rope of 35 m and a codend made of 44-mm diamond stretch mesh equipped with a polyamide codend cover with a 24-mm stretch mesh.

The study area was divided into four regions (Fig. 1): Region 1 (R1) was a fishing zone characterized by unvegetated soft bottoms located close to the city of Antalya (36.8969° N, 30.7133° E) and the main discharge site of the city’s wastewater treatment plant. Region 2 (R2) was also a fishing zone, but the bottom was vegetated by *Posidonia oceanica* (Linnaeus) Delile, 1813 meadows with rocky bottoms and depths less than 35 m (Mutlu & Balaban, 2018). Region 3 (R3) was a non-fishing zone characterized by less vegetation and unvegetated bottoms with steep cliff-like slopes (Mutlu & Balaban, 2018).

There were two transects in R3: one located at the mouth of a river, Manavgat and the other located far from the river to the east. Region 4 (R4) contained extra stations (a bottom depth of 15 m was coded as 10 m, 50 m as 25 m, and 75 m as 75 m) for depth-wise statistical analyses of samples from estuaries of rivers in the mid-study area. Additional stations were trawled perpendic-

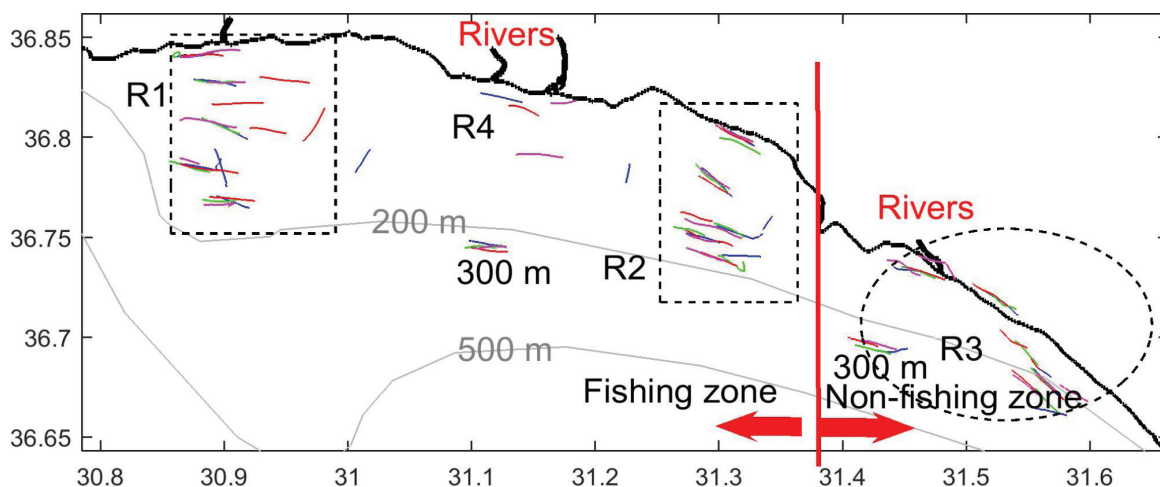


Fig. 1: Study area in red frame with track lines of towing transects by season. (blue = May 2014, green = August 2014, red = October 2014, magenta = February 2015). Standard depths are ordered from shallowest to deepest bottom depth from the coast to open water seaward of each region (R1-R3).

ular to the coast for ground-truthing the fish community observed within a certain depth range fixed on the echogram of the echosounder. One bathyal station (in each of R1-R2 and R3) at 300 m bottom depth was added to each fishing and non-fishing zone to explore succession and extension of pufferfish beyond the shelf in deeper water.

Transects of each region were made perpendicular to the coast and ranged from 10 to 200 m in depth. Each region was transected at 10, 25, 75, 125 and 200 m isobaths. Trawls were towed along the bottom at a speed of 2.5–3 nm for about 30 min. Data from a digital differential global positioning system (DGPS) were recorded during each transect to measure the swept distance.

After each catchment, materials were sorted into liters, benthos, and fish. Fish species were identified on deck when possible, and samples of suspected target species were preserved in 5% formaldehyde for later identification. Sorted species were weighed separately at a precision of 0.01 kg to estimate total biomass of each species. Non-abundant species were counted to calculate their abundance of each species, whereas abundant species were sub-sampled at a ratio of one-third to one-fourth of the total catch. The total length (TL) of each species was measured to produce length-frequency histograms. Specimens present in abundance were preserved in formaldehyde onboard the *R/V Akdeniz Su* for later length measurements at the laboratory. Samples were preserved to establish length-weight relationships for each species and to determine sex composition.

Physical, chemical, optical, and biological variables of the water column and bottom types were determined prior to sampling to establish meaningful ecological parameters. Physical parameters were measured onboard from the sea surface and near-bottom waters collected with a Nansen water bottle to record temperature, salinity, oxygen, and pH using multi-parameter probes (YSI, HiTech); these data were used to calculate water density (σ_t). Half-liter samples of water from the sea surface were filtered through GF/F and GF/C membranes to measure chlorophyll-*a* (chl-*a*) and total suspended matter, respectively; then the filters were frozen for later laboratory work.

Optical parameters were measured using a Secchi disk and an ampoule of photosynthetically active radiation (PAR) from LI-COR (LI-193SA Spherical Quantum Sensor, ampoule and LI-1400 data logger). A Nansen plankton net (70 cm diameter mouth opening and 300 μ m mesh size) was hauled from the bottom to the surface and material were weighed in three size fractions (> 1.0, 0.5, and < 0.063 mm) sorted with a set of sieves. Each size fraction was filtered through a GF/C filter to remove macroplankton and frozen. Acoustical data were recorded to classify bottom types using a scientific echosounder (DT-X, BioSonics, Inc.) operating at a frequency of 200 kHz with a split beam transducer.

At the laboratory, individual total length (mm) and weight (to 0.0001 g) of each species were measured and sexes were determined for individuals. Some individuals were juveniles and could not be sexed; they were recorded as juveniles. Of the environmental parameters, concen-

tration of chl-*a* was measured with a method described by Lorenzen (1967). Total suspended matter was dried in an oven at 60°C for 24 h, and then weighed before the weight of the dried membrane was subtracted from the total dry weight. Samples obtained from the plankton net were then size-fractionated through a sieve series (1, 0.5, 0.063 mm) and each size fraction was filtered on board onto GF/C 25-mm glass-fibre filters. The filter was dried and then burned at 550°C for 5 h at the laboratory. The dry weight was defined as seston, ash weight as tripton, and the difference as bioseston for each fraction. Bottom types were classified as rock, sand, and/or mud as revealed in the acoustical data using a Visual Bottom Typer (VBT, version 1.10.3.5, BioSonics, Inc.) down to 250 m depth. The PAR ampoule was cast from the surface down to 50 m depth using an exponential regression equation extinction rate of PAR estimated for the depth of the water column and the percent light arriving at the seafloor.

Geographical coordinates of DGPS data were recorded at 1-sec intervals and converted to trawling distances. Sweep width (wing spread) of the trawl was factorized by a multiplier of 0.5 with a float-line length as suggested by Pauly (1980) for this type of trawl and region. Abundance (ind/ km²) and biomass (kg/km²) were estimated from the number (*n*) and weight (kg) of individuals in the sweep area using the software MATLAB® (Mathworks Inc.) per haul. The sweep area was calculated using the wing spread of the net (17.5 m) and the start and end point algorithm in MATLAB®.

Statistical analyses were applied to test differences in variables obtained from the species of pufferfish across time, space (depth, region), and sex within species. Three-way analysis of variance (ANOVA) was performed using biomass, abundance, fish total length (TL), fish weight, and sex ratio (female:male) as a function of season, depth, and region. Post-hoc tests (least significant difference, LSD) were applied to each variable independently.

Length-weight (L-W) relationships were tested using analysis of covariance (ANCOVA) for differences in the values of intercepts (*a*) and slopes (*b*) of the power-fit regression equations for each season, depth, region, and species. The constant *b* was tested for significant differences from an isometric constant of $b=3$ for fish using the *t*-student test. Sex composition was the ratio of female: male individuals and was analyzed for differences among seasons, depths, regions, and species. Length frequency was based on bin size estimates from the COST function (Shimazaki & Shinomoto, 2007) for each species. Shimazaki & Shinomoto (2007) underlined that selection of optimal bin size relevant for specific size ranges of each species was of paramount to assess growth cohort. They described that these empirical methods for the bin size selection in a bar graph histogram in an order as follows: i) estimation of the number of sequences required for the histogram, and ii) estimation of the scaling exponents of the optimal bin size were corroborated by theoretical analysis derived for a generic stochastic rate process by dividing the observation period *T* into *N* bins of width Δ from the measurement (iii), and counting the frequency (*ki*) of *i*th bin size (iv), and then constructing the mean

and variance of the number of ki (v) before repeating that computing the cost function changing the bin size Δ to search for minimum $C\Delta^*$ (vi) which is the optimum bin size for the measurement. The kernel density function (KDF) was used to estimate number of cohorts and length ranges of each cohort for each species. Spearman's and Pearson's correlation analyses were used to measure the degree of association between abundance and biomass of the most common species.

All statistical analyses were performed using the statistical tool of MATLAB® (Mathworks Inc.). Canonical correspondence analyses (CCA) were applied to a matrix set of biomass and abundance of species with a corresponding matrix of environmental parameters to cluster the stations and see if relationships between species and ecological parameters can be detected using CANOCA version 4.5.

Results

Six species belonging to the family Tetraodontidae were found in the Gulf of Antalya in the eastern Mediterranean Sea. These species were *Lagocephalus sceleratus* (Gmelin, 1789), *Lagocephalus guentheri* Miranda Ribeiro, 1915, *Lagocephalus suezensis* Clark & Gohar, 1953, *Torquigener flavimaculosus* Hardy & Randall, 1983 *Sphoeroides pachygaster* Hardy & Randall, 1983

and *Tylerius spinosissimus* (Regan, 1908). The dominant species was *L. suezensis*, occurring in high abundance. *L. sceleratus*, *T. flavimaculosus*, and *S. pachygaster* had a similar range with moderate abundance. These species occurred with high frequency, but a regional difference in the distribution of each species was observed. *T. spinosissimus* had the lowest abundance and was found only in the westernmost region of the study area. *T. flavimaculosus* occurred only in R2 and R3, and *S. pachygaster* was present only in deeper zones compared to the other species.

Spearman's correlation analysis was used to measure the degree of association between abundance and biomass of the most common species (Table 1a) and Pearson's correlation coefficients were calculated as well to measure strength of the degree (Table 1b). Abundance and biomass of *Lagocephalus* spp. showed significant correlation with each other, while *T. flavimaculosus* showed significant positive correlation only with *L. suezensis*. The unranked strength of the linear relationship between abundance and biomass was measured using the Pearson product moment correlation coefficient (Table 1b). Abundance and biomass of *L. guentheri* showed significant correlation with abundance of *L. sceleratus*. Abundance and biomass of *L. suezensis* showed significant correlation with biomass of *L. guentheri*. *Torquigener flavimaculosus* showed no significant correlation with any *Lagocephalus* spp.

Table 1. Correlations (A, Spearman and B, Pearson) of biomass (B) and abundance (A) of four common pufferfish. Black numbers indicate correlation coefficients and red numbers significance levels (p value). Bold coefficients were significant at $p < 0.05$ ($n = 79$).

		<i>L. sceleratus</i>		<i>L. guentheri</i>		<i>L. suezensis</i>		<i>T. flavimaculosus</i>	
A		B	A	B	A	B	A	B	A
<i>L. sceleratus</i>	B	1.000	0.990	0.525	0.514	0.360	0.357	0.009	0.014
	A	0.000	1.000	0.540	0.529	0.369	0.370	0.007	0.013
<i>L. guentheri</i>	B	0.000	0.000	1.000	0.998	0.552	0.540	-0.042	-0.023
	A	0.000	0.000	0.000	1.000	0.555	0.544	-0.038	-0.019
<i>L. suezensis</i>	B	0.001	0.001	0.000	0.000	1.000	0.996	0.413	0.418
	A	0.001	0.001	0.000	0.000	0.000	1.000	0.416	0.422
<i>T. flavimaculosus</i>	B	0.937	0.952	0.713	0.737	0.000	0.000	1.000	0.997
	A	0.903	0.909	0.840	0.866	0.000	0.000	0.000	1.000
B									
<i>L. sceleratus</i>	B	1.000	0.603	0.263	0.014	-0.035	-0.037	-0.052	-0.057
	A	0.000	1.000	0.526	0.412	0.040	0.233	-0.072	-0.057
<i>L. guentheri</i>	B	0.019	0.000	1.000	0.866	0.546	0.487	-0.086	-0.046
	A	0.899	0.000	0.000	1.000	0.263	0.246	-0.063	-0.007
<i>L. suezensis</i>	B	0.760	0.728	0.000	0.019	1.000	0.851	-0.031	-0.032
	A	0.746	0.039	0.000	0.029	0.000	1.000	-0.040	-0.044
<i>T. flavimaculosus</i>	B	0.647	0.531	0.452	0.581	0.788	0.724	1.000	0.855
	A	0.615	0.620	0.686	0.951	0.778	0.701	0.000	1.000

Lagocephalus sceleratus

Lagocephalus sceleratus was found at seafloor depths of 10, 25, and 75 m in all regions. The highest biomass was 135 kg/km² in February and the highest abundance was 150 ind/km² in October and February, particularly obvious in R1 (Fig. 2). Populations were dominated by males May–October, while females were abundant mainly in February.

Biomass did not differ significantly among regions, seasons, and bottom depths (ANOVA, $p = 0.675, 0.373, \text{ and } 0.780$, respectively). The highest biomass was highest in R1 ($X \pm SD: 5.43 \pm 3.10 \text{ kg/km}^2$) and lowest in R3 ($0.03 \pm 3.16 \text{ kg/km}^2$, Fig. 2). Biomass increased from a minimum in May ($0.13 \pm 3.34 \text{ kg/km}^2$) and August ($0.46 \pm 3.79 \text{ kg/km}^2$) to a maximum in October ($1.74 \pm 3.41 \text{ kg/km}^2$) and February ($7.97 \pm 3.59 \text{ kg/km}^2$). Biomass increased with depth: $0.97 \pm 4.12 \text{ kg/km}^2$ at 10 m, $3.69 \pm 4.43 \text{ kg/km}^2$ at 25 m and $9.72 \pm 4.27 \text{ kg/km}^2$ at 75 m (Fig. 2A).

Abundance of *L. sceleratus* did not differ significantly among regions, seasons (months), and depths ($p = 0.252, 0.215, \text{ and } 0.269$, respectively). Maximum abundance was found in R1 ($17.35 \pm 5.28 \text{ ind/km}^2$) and R4 (13.20

$\pm 12.04 \text{ ind/km}^2$) and minimum abundance in R2 ($3.43 \pm 5.61 \text{ ind/km}^2$) and R3 ($4.92 \pm 5.38 \text{ ind/km}^2$). Abundance increased gradually from May ($1.77 \pm 5.73 \text{ ind/km}^2$) through August ($3.88 \pm 6.51 \text{ ind/km}^2$), and experienced abrupt spikes in October ($13.90 \pm 5.86 \text{ ind/km}^2$) and February ($16.95 \pm 6.16 \text{ ind/km}^2$). In contrast to biomass, abundance decreased with depth from $20.40 \pm 6.91 \text{ ind/km}^2$ at 10–25 m to $11.36 \pm 7.16 \text{ ind/km}^2$ at 75 m (Fig. 2B).

Sex ratios did not differ significantly among regions, seasons, and depths ($p = 0.338, 0.718, \text{ and } 0.909$, respectively); however, an increase in p values from west (0.09 ± 0.22) to east (1.00 ± 0.44) was observed suggesting strength of dominance of the females. Females were mostly absent in May and August, whereas the ratio of females:males was twice as high in October (0.50 ± 0.25) than in February. The ratio had the same value at 10 and 25 m ($0.34 \pm 0.29 - 0.33 \pm 0.29$) and the lowest value at 75 m (0.16 ± 0.36 , Fig. 2C).

The total length of *L. sceleratus* varied between 5.4 and 62.5 cm. The COST function estimated an optimum length class interval (i.e., bin size) of 14.28 cm. More than half of the total number of fish were longer than 15 cm. The KDF assessed three cohorts from the total length

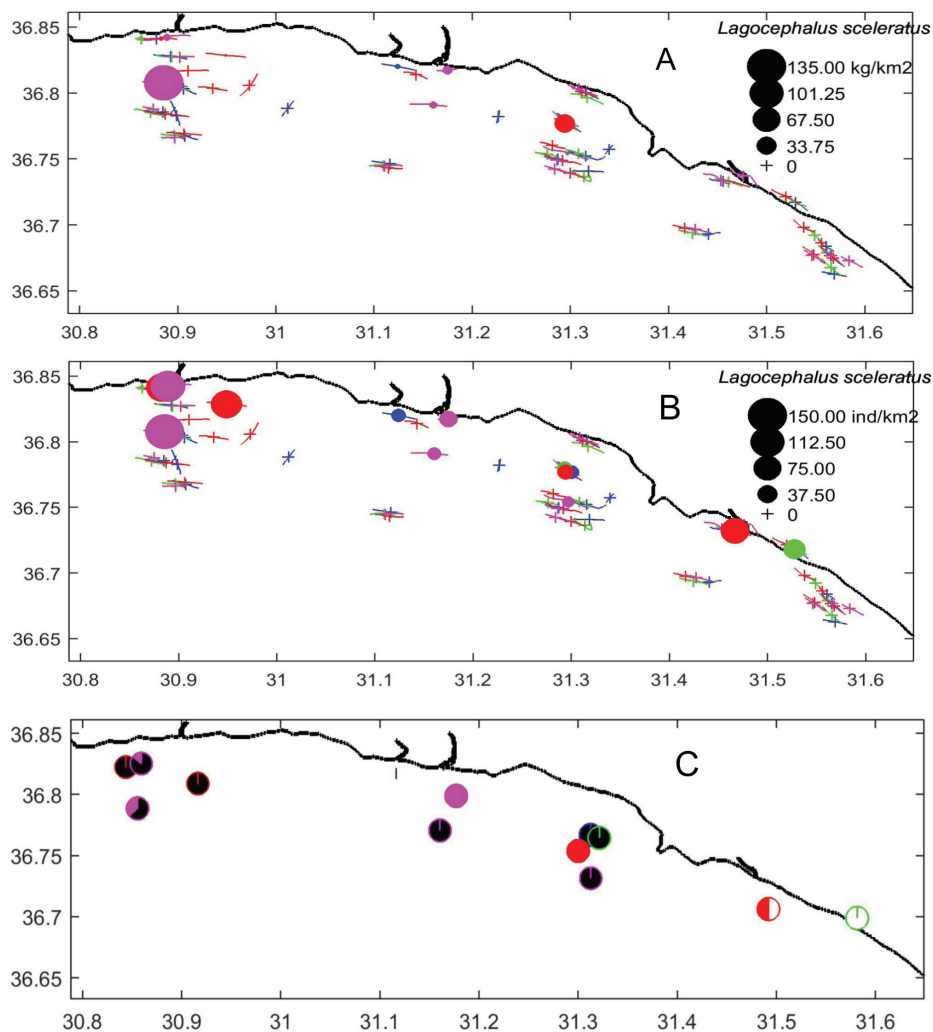


Fig. 2: Distribution of (A) biomass, (B) abundance (circles square-rooted), and (C) percent sex ratio of *Lagocephalus sceleratus* in time (months) and space (regions and depths). Seasonal colors on the figures are: blue for May 2014, green for August 2014, red for October 2014, and magenta for February 2015. Colors for sex ratio: females follow seasonal color scheme, males are black, and juveniles are white in seasons.

frequency histograms. The number of cohorts was fixed at four size classes (< 20, 20–33, 33–50, and > 50 cm); one class had no length measurements because the bin size increased to 30 classes. The length differed significantly among seasons, depths, and sexes but not regions ($p = 0.019, 0.0001, 0.0002, \text{ and } 0.103$, respectively); however, post-hoc tests showed that mean lengths were significantly smaller (7.03 ± 5.80 cm) in R3 than in the other regions (20 cm in R1, 29 cm in R2, and 25 cm in R4) which were not significantly different from each other. The length in February was significantly longer (25.12 ± 2.83 cm) than that in October (10.63 ± 3.39 cm). The lengths in the pairs between other seasons were not significant between seasons (TL; 15 and 18 cm). The total length was significantly longer (33.03 ± 3.51 cm) at 75 m bottom depth than similar lengths (13.24 ± 3.25 cm) at the other two depths (10 and 25 m). Lengths of female individuals were significantly longer (36.16 ± 4.23 cm) than that of males (18.27 ± 2.49 cm).

Individual weights of the fish ranged from 2.04 to 3700 g during the year. There were significant differences in weights among bottom depths and sex ($p = 0.004$ and 0.001 , respectively). There were no significant differences in individual weights by region. The weights varied between a minima (5.26 ± 299.02 g) in R3 and a maxima (440.81 ± 366.22 g) in R2. The increase in individual weights did not increase significantly from 65.51 ± 50.59 g in May to $88\text{--}94$ g in August–October to 481.05 ± 149.20 g in February. However, the weights were significantly heavier (855.64 ± 185.22 g) at depth (75 m) than the weights (39–143 g) at coastal depths (10–25 m). Individual mean weights of females were significantly higher (1168.5 ± 213.15 g) than that of males (149.44 ± 125.71 g).

Length-weight (L-W) relationship was estimated for males, females, and pooled data (Fig. 3). Fish showed isometric growth ($b = 2.89$) because the slopes were not significantly different from the constant ($b = 3$) for males,

females, and remaining individuals ($n = 44$, student $t = -0.075$; $n = 30$, $t = -0.279$, and $n = 8$, $t = -0.160$, respectively). The length-weight relationship was not significantly different between sexes (ANCOVA, $p = 0.307$). There was no significant difference in the length-weight regressions among regions (mean \log_{10} -transformed intercept, $a = -1.66 \pm 0.15$ ($X \pm SE$) and slope, $b = 2.79 \pm 0.13$). Slope and intercepts of the regression changed significantly with seasons and bottom depths ($p = 0.005$ and 0.019 , respectively). The slopes were 3.447, 2.847, 2.791, and 3.032 in R1, R2, R3, and R4, respectively, whereas the intercepts were 0.0031, 0.0163, 0.022, and 0.0111, respectively. The slopes were 2.827 at 10 m bottom depth, 2.787 at 25 m, and 3.004 at 75 m depth and the intercepts were 0.0189, 0.0226, and 0.0125, respectively.

Lagocephalus guentheri

The species *L. guentheri* was found between 10 and 75 m seafloor depth. The maximum biomass was 25 kg/km² and maximum abundance was 690 ind/km² (Fig. 4). With the exception of R2 which only had one occurrence, the species was frequently found in the other regions and seemed to decrease from west to east across the study area.

Regional differences were observed for the biomass of *L. guentheri* (ANOVA, $p = 0.002$). The mean biomass was significantly higher in R4 (7.94 ± 1.79 kg/km²), seaward of the river mouths. R2 had the least biomass (0.02 ± 0.83 kg/km²), and the other regions varied between 0.73 ± 0.80 kg/km² in R3 and 1.61 ± 0.78 kg/km² in R1. The biomass did not differ significantly with season ($p = 0.27$); however, the biomass increased from May (0.17 ± 0.92 kg/km²) through August–to–October (0.68 ± 1.04 to 1.59 ± 0.94 kg/km²) to February (2.72 ± 0.99 kg/km²). The species was found at depths of bottom of 10–25 m and 75 m during the year (Fig. 4) and showed no signifi-

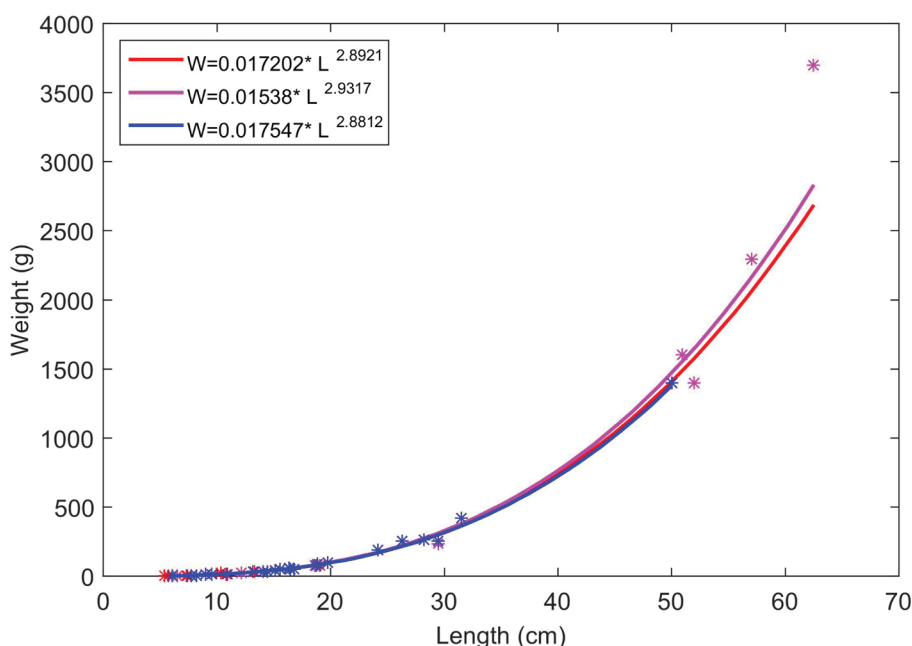


Fig. 3: Length-weight relationships of males (blue), females (pink), and pooled data (red) of *Lagocephalus sceleratus*.

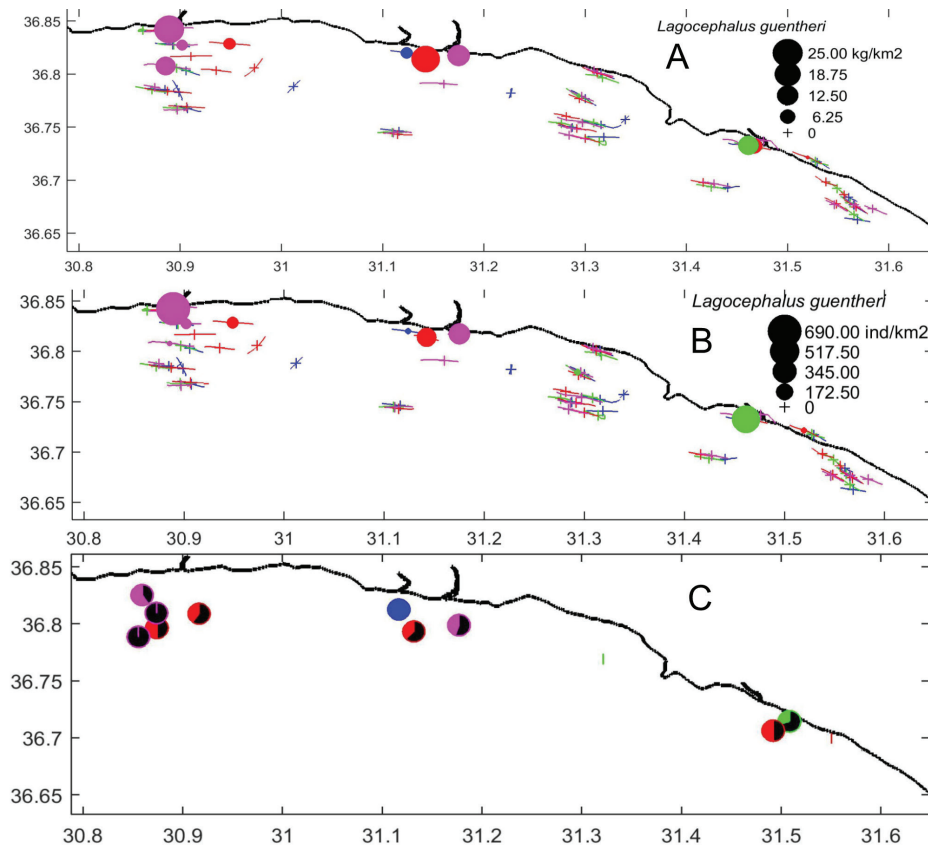


Fig. 4: Distribution of (A) biomass, (B) abundance (circles square-rooted), and (C) percent sex composition of *Lagocephalus guentheri* in time (months) and space (regions and depths). Seasonal colors on figures are: blue = May 2014, green = August 2014, red = October 2014, and magenta = February 2015. Colors for sex ratio: females follow seasonal color scheme, males are black, and juveniles are white in seasons.

cant differences in biomass as a function of bottom depth ($p = 0.135$). The biomass decreased with bottom depth and was only significantly higher at 10 m (4.28 ± 1.09 kg/km²) than at 75 m (0.76 ± 1.13 kg/km²).

Unlike biomass, abundances were not statistically different among regions (ANOVA, $p = 0.221$). The minimum abundance was 0.91 ± 20.66 ind/km² in R2 and the maximum abundance 101.80 ± 44.32 ind/km² in R4. Region R3 had an abundance of 23.32 ± 19.82 ind/km² and R1 had 32.23 ± 19.44 ind/km². There was no significant difference in the abundance among seasons ($p = 0.404$). Minimum abundance was estimated in May at 0.86 ± 21.34 ind/km², while maximum abundance occurred in February (54.05 ± 22.96 ind/km²). Abundance was 28.71 ± 24.27 ind/km² in August and 19.86 ± 21.84 ind/km² in October. Differences in abundance as a function of bottom depth was not statistically significant ($p = 0.250$); however, abundance in shallow waters was significantly higher (80.87 ± 25.46 ind/km²) than in deep waters (0.93 ± 26.36 ind/km²), and the abundance at 25 m was 55.77 ± 27.35 ind/km².

Sex ratios did not change significantly among regions, seasons, and bottom depths ($p = 0.875, 0.865, \text{ and } 0.188$, respectively). Regions 1 and 4 had higher ratios (0.66 ± 0.39 each) than R3 (0.34 ± 0.54). The ratios increased linearly from August (0.18 ± 0.80) to May (1.00 ± 0.80) with a difference of 0.25 between seasons. With respect to bottom depth, the ratios varied between 1.00 ± 0.29 at

10 m and 0.28 ± 0.29 at 25 m.

The total length of *L. guentheri* varied between 7 and 25.2 cm during the year. The COST function estimated an optimum size class interval of 0.43 cm. Five cohorts were fixed using the KDF to estimate the density of each cohort corresponding to minimum densities, ranging from <8.5, 8.5–14, 14–17, 17–19, and >19 cm. Cohort 2 dominated the population, followed by cohort 3. The lengths were significantly different among regions, seasons, bottom depths, and sex ($p = 1.0 \times 10^{-8}, 6.8 \times 10^{-6}, 0.0006$, and 0.0031, respectively). The minimum length (12.69 ± 0.33 cm) was found in R2 and the maximum length (15.88 ± 0.59 cm) was found in R4. The length was not significantly different between R1 (9.26 ± 0.86 cm) and R3 (11.92 ± 0.49 cm). The lengths were significantly longer (24.10 ± 2.73 cm) in May than in other seasons and were not significantly different between October (13.72 ± 0.52 cm) and February (12.78 ± 0.34 cm) whereas the minimum lengths were significantly different in August (11.00 ± 0.58 cm). The length decreased from bottom depths of 10–25 m ($13\text{--}12 \pm 0.43$ cm) to 50 m (8.98 ± 1.01 cm), and the longest individuals were observed at bottom depths of 75 m (15.30 ± 2.84 cm). Length (10.81 ± 0.68 cm) was significantly different by sex. Post-hoc tests showed no significant differences between the total length of females (13.55 ± 0.42 cm) and males (12.79 ± 0.42 cm).

Individual weight differed significantly among re-

gions, seasons, and sex including pooled sexes ($p = 2.9 \times 10^{-6}$, 5.0×10^{-8} , and 0.0203, respectively). Individuals were significantly heavier in R4 (83.37 ± 8.19 g) than in the other regions, ranging from 21.97 ± 11.90 g in R2 to 37.91 ± 4.53 g in R1; the latter two did not differ significantly from each other. Similar to length, weight was highest (220.91 ± 34.42 g) in May and lowest (21.19 ± 7.34 g) in August. October and February did not differ significantly in weight (60.06 ± 6.50 g and 38.98 ± 4.24 g, respectively), and weight was not significantly different between bottom depths of 50 m (21.89 ± 14.01 g) and 75 m (65.84 ± 39.62 g). Shallow waters had fish of moderate weight (~ 40 g/ind.). The difference in weight did not differ significantly between males (40.42 ± 5.58 g) and females (52.22 ± 5.64 g).

The length-weight relationship was significantly different for females, males, and pooled individuals (Fig. 5). The slopes of the regression lines were significantly different from the isometric growth value of 3 ($n = 112$, $t = -2.455$) for all individuals but not for the males and females ($n = 49$, $t = -1.474$ and $n = 48$, $t = -1.991$) at $p < 0.05$, resulting in negative allometric growth for the individuals. Overall, there was a significant difference in length-weight regression constants among regions, bottom depths, and sex owing to the contribution from individuals of undefined sex ($p = 0.041$, 0.044, and 0.038, respectively).

Estimates of slopes and intercepts among regions were statistically similar between R1 (2.724 and 0.0355, respectively) and R2 (3.065 and 0.0471, respectively), and between R3 (3.085 and 0.0125, respectively) and R4 (2.916 and 0.0218, respectively). The slope was significantly higher in R3 than in R2 whereas the intercept was significantly lower in R3 than R2. There were no significant differences in L-W regressions among seasons. Only the intercepts differed significantly between bottom

depths of 25 m (0.0124) and 50 m (0.0420), and one individual was found in regions with bottom depths of 75 m. The L-W relationships were not significantly different between females and males (Fig. 5).

Lagocephalus suezensis

The most invasive species, *L. suezensis*, were abundant at all shelf stations with bottom depths of 10–to-125 m (Fig. 6). Maximum average biomass was 300 kg/km² (Fig. 6A), and maximum abundance was $11,024$ ind/km² (Fig. 6B). This species was abundantly present in all regions, particularly in R4.

Regional differences were determined statistically for biomass distribution ($p = 0.012$). This difference was due to much higher biomass in R4 (62.95 ± 16.31 kg/km²) than in the other regions (2.75 – 10.09 ± 7.40 kg/km², Fig. 7A). The biomass was significantly different among seasons and bottom depths ($p = 0.448$ and 0.269, respectively). Seasonal biomass varied from 1.59 ± 9.34 kg/km² in August to 19.57 ± 8.41 kg/km² in October (Fig. 7B). Biomasses were tended to decrease from shallower waters (24.32 – 30.62 ± 10.04 kg/km²) to deep waters (< 2.00 kg/km²) (Fig. 7C). Depths greater than 125 m were virtually devoid of *L. suezensis*.

Overall, there were no significant differences in abundance among regions, seasons, and bottom depths ($p = 0.084$, 0.191, and 0.133, respectively, Fig. 6B). Abundance was significantly higher (2294.60 ± 762.64 ind/km²) in R4 than in the other regions (from 119.26 ± 355.58 ind/km² in R2 to 573.61 ± 334.44 ind/km² in R1). Maximum mean abundance occurred in October (1157.20 ± 376.87 ind/km²), while minimum abundance occurred in August (56.24 ± 418.87 ind/km²). Abundance decreased with bottom depth from high abundance in shallower

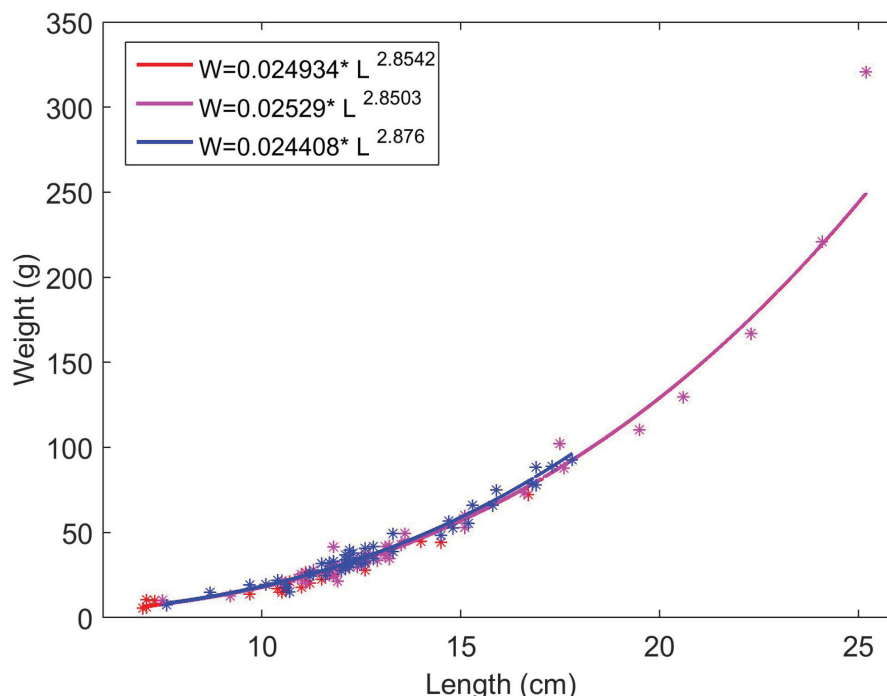


Fig. 5: Length-weight relationships of males (blue), females (pink), and pooled data (red) of *Lagocephalus guentheri*.

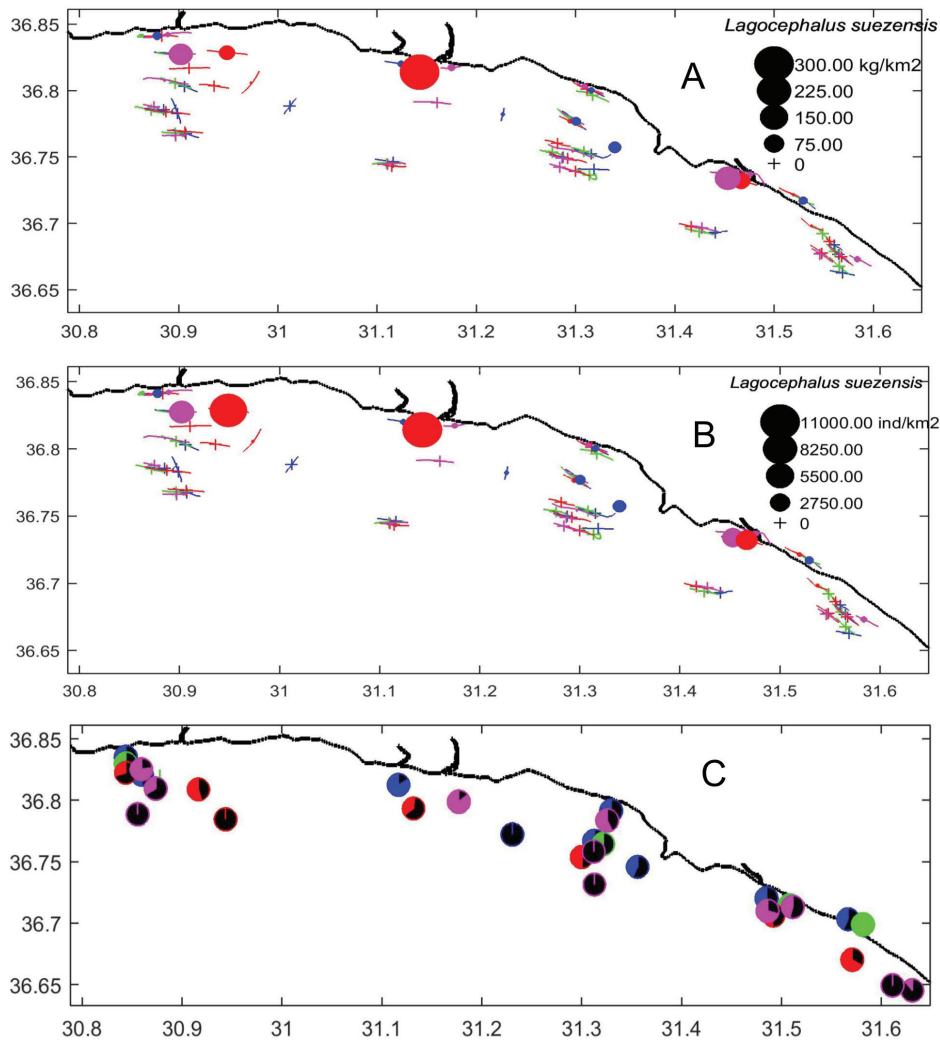


Fig. 6: Distribution of (A) biomass, (B) abundance (circles square-rooted), and (C) percent sex composition of *Lagocephalus suezensis* in time (months) and space (regions and depths). Seasonal colors on the figures are: blue = May 2014, green = August 2014, red = October 2014, and magenta = February 2015. Colors for sex composition: females follow seasonal color scheme, males are black, and juveniles are white in seasons.

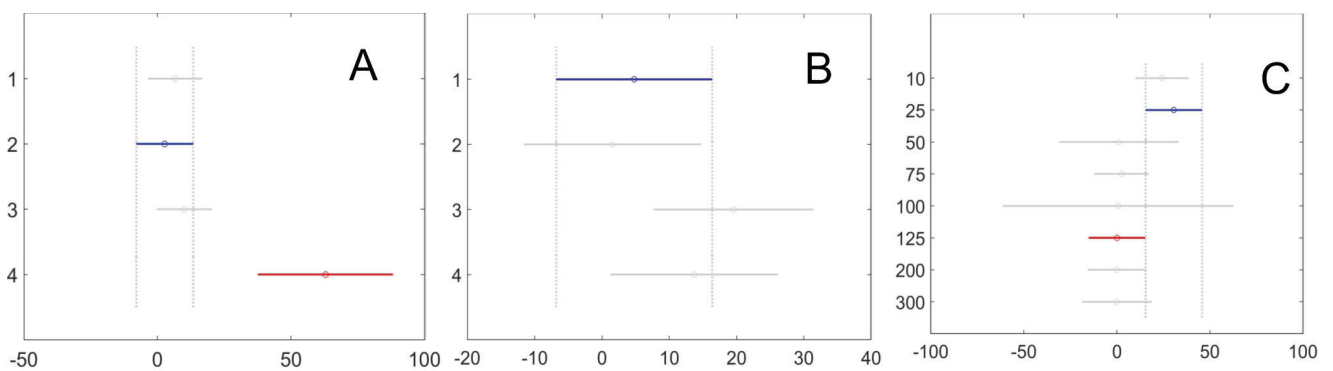


Fig. 7: Post-hoc test (least significant difference, LSD) of biomasses in kg/km² of *Lagocephalus suezensis* among (A) regions, (B) seasons (1 = May, 2 = August, 3 = October, and 4 = February), and (C) bottom depths. Circle = mean, horizontal bar = standard deviation, blue mark = to be tested for biomasses among regions, months and depths, red = significant difference, gray = no significant difference between vertical discrete gray lines.

waters (> 1000 ind/km² from 10 to 25 m and low abundance at greater depths (< 100 ind/km² from 50–125 m).

Dominance of females over males did not differ among regions, seasons, and bottom depths ($p = 0.611$, 0.091, and 0.925, respectively). Regions R1 and R2 had

sex ratios < 2, whereas the ratios were higher in R3 (58.95 ± 33.85) and R4 (20.43 ± 61.79). The ratio was significantly higher (144.50 ± 49.03) in August than in the other seasons. Females predominated in bottom depths of 25 m (53.34 ± 33.82), then decreased to 0.14 ± 56.09 at 75 m;

thereafter, no females were observed in the seaward direction.

Total length of *L. suezensis* varied between 4 cm and 18.5 cm during the year (Fig. 8A). The COST function estimated an optimum size class (bin size) of 0.52 cm for total length distribution of the species (Fig. 8B). The KDF determined five cohorts in total length: 4.0–5.5, 5.5–10.2, 10.2–14.3, 14.3–17.0, and > 17 cm (Fig. 8A). The third cohort was the dominant cohort in the population.

The lengths of the species were significantly different among regions, seasons, bottom depths, and sex ($p = 1.3 \times 10^{-14}$, 2.5×10^{-19} , 2.0×10^{-9} , and 2.2×10^{-27} , respectively). The lengths were significantly shorter in R1 (10.21 ± 0.19 cm) than the other regions (11.91 ± 0.18 to 12.44 ± 0.22 cm) (Fig. 9A). The shortest lengths differed significantly in October (10.59 ± 0.14 cm) and the longest individuals were present in February (13.01 ± 0.26 cm) (Fig. 9B). The lengths were significantly longer at bottom depths of 75 m (12.64 ± 0.44 cm) than lengths in bottom depths of 25 m (10.79 ± 0.15 cm) and 50 m (10.26 ± 1.13 cm, Fig. 9C). Females were significantly longer (12.37 ± 0.15 cm) than males (11.35 ± 0.14 cm); however, lengths of 8.35 ± 0.40 cm could not be sexed, and juveniles were 4.93 ± 0.96 cm in length (Fig. 9D).

Individual weight varied between 1.10 and 82.73 g. The weight changed significantly with the regions, seasons, bottom depths, and sex ($p = 2.8 \times 10^{-11}$, 4.1×10^{-16} , 5.6×10^{-6} and 7.5×10^{-20} , respectively). Individuals were significantly heavier in R4 (27.50 ± 1.13 g) than in R1 (16.88 ± 1.01 g) and R2 (23.17 ± 1.52 g). The weight in May (25.39 ± 1.07 g) was significantly higher than in October (18.32 ± 0.75 g) and lower than in February (29.97 ± 1.35 g). Individuals were significantly lighter in weight in bottom depths of 25 m (19.59 ± 0.81 g) than at 10 m (25.64 ± 0.83 g) and 75 m (26.78 ± 2.34 g). Females were heavier (27.40 ± 0.81 g) than males on average (20.88 ± 0.75 g).

The total length relationship with weight of *L. suezensis* regressed significantly for the females, males, and

total individuals (Fig. 10). The slopes of the regression lines were not significantly different from the isometric slope of 3 for total and female individuals, but significantly different for males ($n = 522$, $t = -1.761$; $n = 280$, $t = -2.138$; $n = 239$, $t = -1.928$, respectively) at $p < 0.05$. This species grew in an isometric type of length-weight relationship.

Constants for the length-weight regression equations were significantly different by regions, bottom depths, and sex, including juveniles and individuals of undefined sex ($p = 5.0 \times 10^{-7}$, 0.0022, and 0.0008, respectively); there was no significant difference among the seasons. The slopes and intercepts were not significantly different between males and females at $p < 0.05$. The slope was significantly lower in R2 than in the other regions, whereas they were not significant in R1 and R3 (Table 2). Regional differences were not estimated by post-hoc tests for length-weight relationships. Like the differences among sex (excluding undefined sex and juveniles), depth-wise differences in slopes and intercepts of length-weight relations were not significantly different; greater depths were excluded due to insufficient number of *L. suezensis* individuals.

Torquigener flavimaculosus

The species *T. flavimaculosus* was found mostly in the eastern part of the study area. The species was not found in R4 located in front of the river. This species was distributed on the shelf without exceeding bottom depths of 75 m, the maximum biomass was 2 kg/km², and the abundance was 150 ind/km² in the other regions (Fig. 11). The biomass of the species was not significantly different among regions, seasons, and bottom depths ($p = 0.190$, 0.306, and 0.077, respectively); however, the mean biomass was significantly higher in R3 (0.20 ± 0.06 kg/km²) than in R1 (0.03 ± 0.06 kg/km²). The seasonal biomass varied between 0.037 ± 0.08 kg/km² in August and 0.20

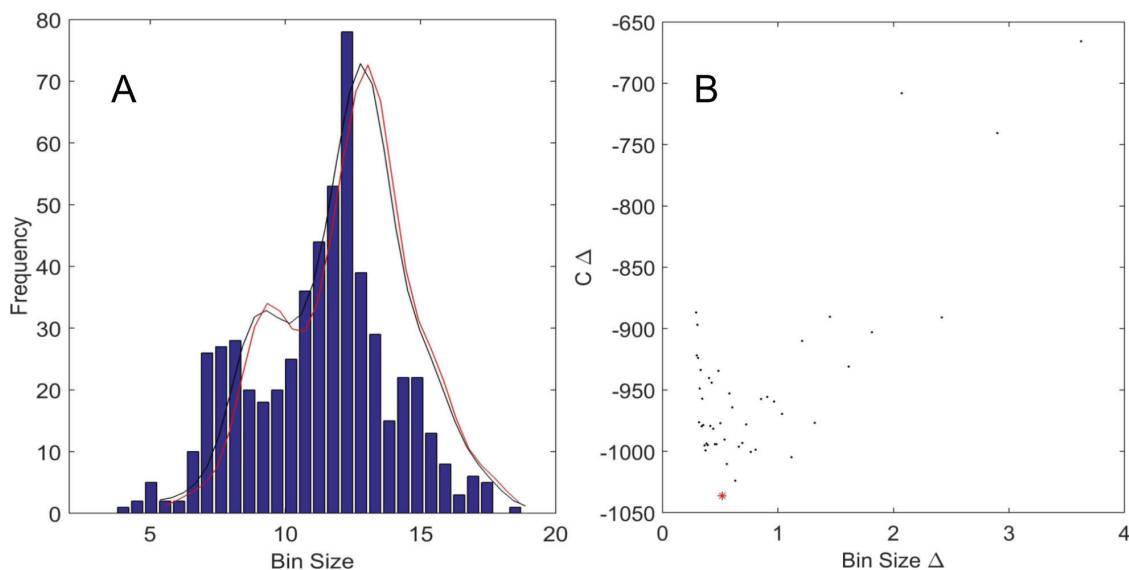


Fig. 8: *Lagocephalus suezensis*: (A) length-frequency histogram with solution of the KDF in a size class interval estimated by (B) COST function. Asterisk * = optimum length class interval in cm.

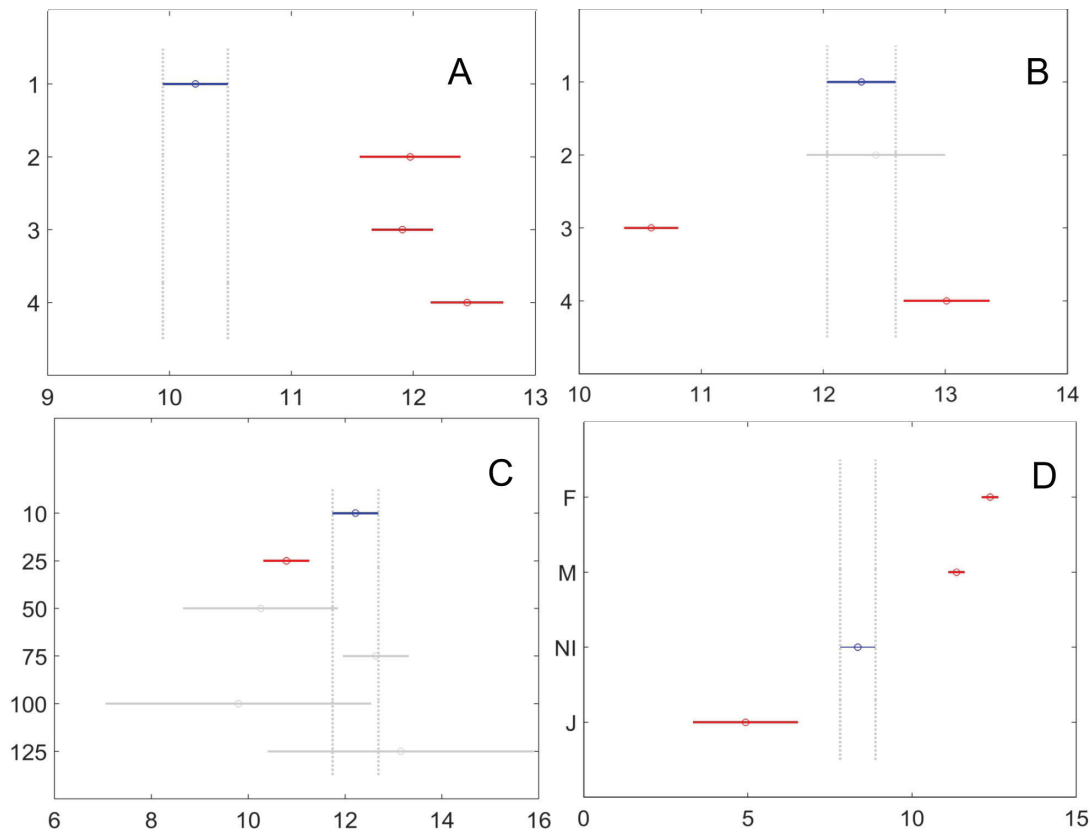


Fig. 9: Post-hoc test (least significant difference, LSD) in total length in cm of *Lagocephalus suezensis* among (A) regions, (B) seasons (1 = May, 2 = August, 3 = October, and 4 = February), (C) bottom depths, and (D) sex (F = female, M = male, NI = sex not identified, and J = juvenile). Circle = mean, horizontal bar = standard deviation, blue mark = to be tested among the regions, months, and depths, red = significantly different, gray = not significantly different between vertical discrete gray lines.

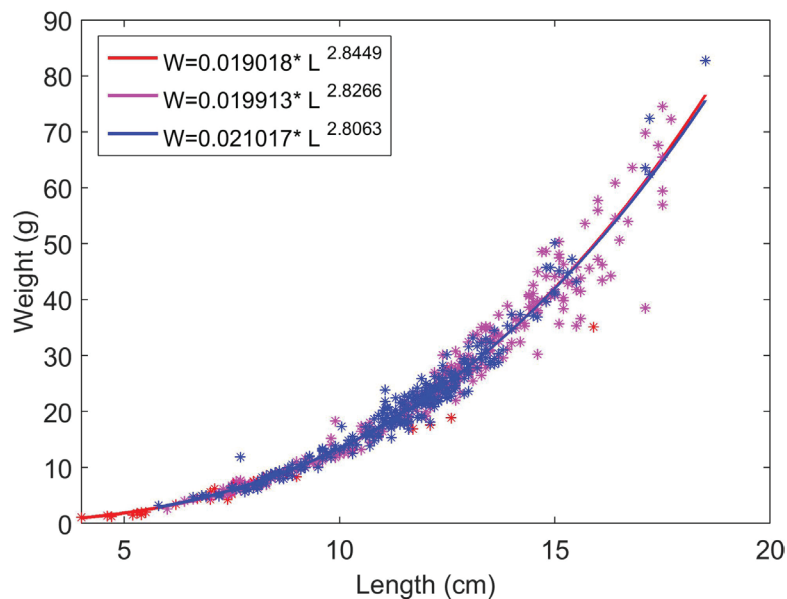


Fig. 10: Length-weight relationships of males (blue), females (pink), and pooled data (red) of *Lagocephalus suezensis*.

$\pm 0.07 \text{ kg/km}^2$ in May. The biomass decreased slightly with bottom depths of 50 m, and then was higher at 75 m ($0.35 \pm 0.08 \text{ kg/km}^2$) only than that at 25 m ($0.10 \pm 0.08 \text{ kg/km}^2$, Fig. 11A).

Results of ANOVA showed that abundance did not differ significantly among regions, seasons, and bottom depths ($p = 0.160, 0.503, \text{ and } 0.063$, respectively). Never-

theless, the mean abundance was significantly higher in R3 ($21.24 \pm 5.65 \text{ ind/km}^2$) than in R1 ($4.96 \pm 5.54 \text{ ind/km}^2$). The maximum seasonal abundance was estimated to be $16.77 \pm 6.14 \text{ ind/km}^2$ in May, and the minimum abundance was $4.18 \pm 6.98 \text{ ind/km}^2$ in August. Similar to biomass distribution by bottom depth, abundance varied between 7.69 and 8.33 ind/km^2 at 25–50 m, 26.53 ind/km^2 at 10 m, and

Table 2. Estimates of coefficient estimates of length-weight regression equations for *Lagocephalus suezensis* among regions and t-tests representing the coefficients (slopes and \log_{10} -transformed intercepts) of power-fit regression line. Bold *p* values are significant and representative of slopes and intercepts in the equations.

Term	Estimate	Std. Err.	<i>t</i>	<i>p</i>
Intercept	-1.686	0.0264	-63.68	1.6*10⁻²⁵⁶
1	-0.058	0.0340	-1.72	0.0855
2	0.312	0.0673	4.64	4.2*10⁻⁶
3	-0.034	0.0328	-1.03	0.3012
4	-0.220	0.0405	-5.43	8.0*10⁻⁸
Slope	2.814	0.0247	113.78	0.0000
1	0.068	0.0326	2.09	0.0367
2	-0.289	0.0626	-4.62	4.7*10⁻⁶
3	0.021	0.0307	0.71	0.4789
4	0.199	0.0374	5.33	1.4*10⁻⁷

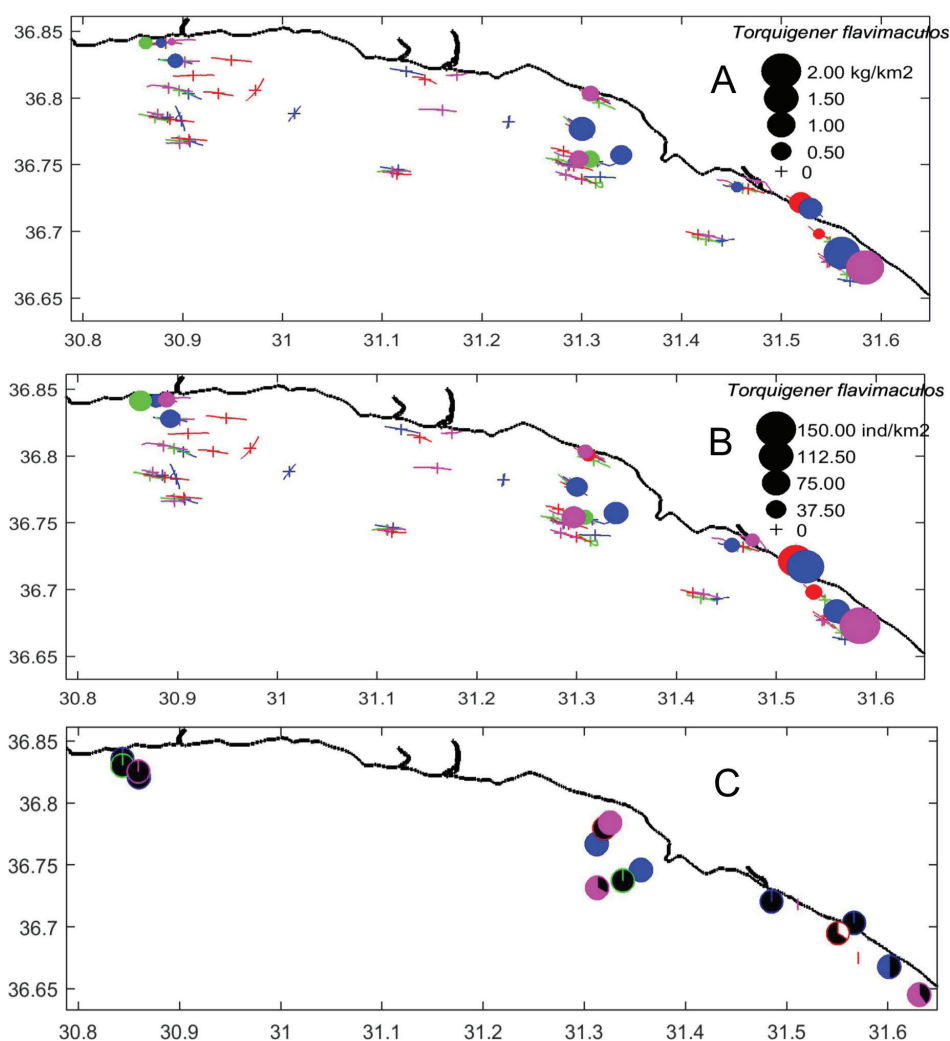


Fig. 11: Distribution of (A) biomass, (B) abundance (circles square-rooted), and (C) percent sex composition of *Torquigener flavimaculosus* in time (months) and space (regions and depths). Seasonal colors on the figures are: blue = May 2014, green = August 2014, red = October 2014, and magenta = February 2015. Colors for sex composition are: females follow seasonal color scheme, males = black, and juveniles = white in seasons.

25.14 ind/km² at 75 m (Fig. 11B).

Dominance of females over males was not significant among regions, seasons, and bottom depths ($p = 0.291$, 0.094 , and 0.081 , respectively). The female:male ratio varied seasonally between $3.3 \times 10^{-16} \pm 0.55$ by male dominance in R1 and 1.16 ± 0.45 by female dominance in R2. The ratio was significantly higher in February (1.81 ± 0.48) than in May (0.36 ± 0.37). In the other seasons, females were mostly absent with males present in high abundance. Greater bottom depths (75 m) had higher abundances of females (1.55 ± 0.44) as compared to males.

The total length (TL) of *T. flavimaculosus* ranged from 3.6 to 11.1 cm in the study area. The optimum length class interval was estimated to be 1.07 cm for the length distribution; however, one cohort (3.6–11.1 cm in TL) was estimated. The length changed significantly with bottom depth and sex ($p = 0.037$ and 4.5×10^{-5} , respectively). Regional length distributions varied between 6.02 ± 0.80 cm in R1 and 8.07 ± 0.62 cm in R2. Seasonally, the maximum length was 7.95 ± 1.43 cm in August and the minimum length was 6.28 ± 0.72 cm in October. The specimens were significantly longer at bottom depths of 75 m (8.16 ± 0.50 cm) than at 10 m (6.27 ± 0.43 cm). Female individuals were significantly longer (8.94 ± 0.48 cm) than males (7.18 ± 0.33 cm). Specimens with lengths less than 5.0 cm could not be sexed.

Similar to length distribution, individual weights were significantly different with respect to bottom depth and sex ($p = 0.010$ and 0.001 , respectively). There were no significant seasonal or regional differences in weight. There were light individuals in R1 (5.35 ± 2.82 g) and in October (5.76 ± 2.51 g) and heavy individuals in R2 (12.43 ± 2.18 g) and in May and August (~ 11 g). There were significantly heavier individuals at bottom depths of 25 m and 75 m (~ 13 g) than at 10 m (5.56 ± 1.44 g). Females were significantly heavier (15.74 ± 1.83 g) than males (8.25 ± 1.23 g). Individuals that weighed less than 3 g could not be sexed.

Length-weight relationships did not differ significantly by region, season, bottom depth, and sex ($p = 0.050$,

0.517 , 0.803 , and 0.342 , respectively). Regression equations of L-W relationships are shown in Figure 12 for females, males, and total individuals pooled. The species showed significant isometric growth in length with the weights for the all individuals, males, and females ($n = 33$, $t = 0.012$; $n = 22$, $t = -0.347$, and $n = 10$, $t = 0.101$, respectively) at $p < 0.05$.

Sphoeroides pachygaster

One of two rare species belonging to the family Tetraodontidae was *S. pachygaster*, found at two trawl stations. This species was caught only at bottom depths of 200 m in October (R2) and February (R1). The maximum biomass was estimated to be 30 kg/km² with the maximum abundance of 120 ind/km² in February (R1), which is higher than in October (16 kg/km² and 20 ind/km², respectively). The number of males was 16 ind/km² in February. The number of females varied between 20 ind/km² in October and 36 ind/km² in February. Lengths ranged from 12.0 to 30.4 cm, whereas individual weights varied from 48.43 to 600 g. Males were shorter than 15 cm, with weights of 50–60 g and females were 15–30 cm long and weighed between 100 and 600 g. Statistical significance of the measurements was not expected to test the differences among the regions, seasons, and bottom depths because the number of individuals was insufficient (only two males and four females in the catch) to establish L-W relationships, but six individuals could be useful to establish L-W significant regression lines for total specimens ($W = 0.060334L^{2.6995}$) of this rare species (unpublished data).

Tylerius spinosissimus

Tylerius spinosissimus was found only in R1 at bottom depths of 50 m in October and 75 m in February. In total, three individuals were caught. The biomass varied between 0.02 kg/km² in February and 0.05 kg/km² in October

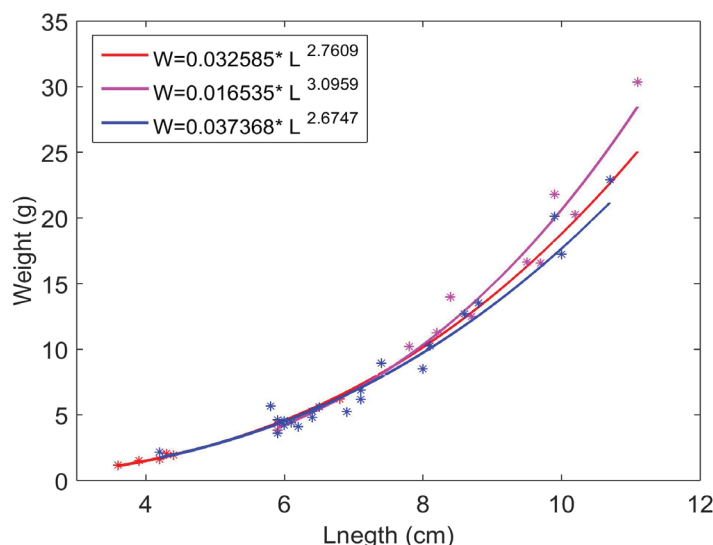


Fig. 12: Length-weight relationships of males (blue), females (pink), and unisex pooled data (red) of *Torquigener flavimaculosus*.

with abundance ranging from 31 ind/km² and 13 ind/km², respectively. Length varied between 3.4 and 4.7 cm and weight ranged between 0.84 and 2.41 g. It was not possible to identify sex.

Species distribution-environmental parameter relations

Abundance and biomass of all species were discriminated by bottom depths on the first CCA axis with an explained variance of 53.6% (Fig. 13). Most of the species were positively correlated with chl-*a* and biological parameters (tripton, seston, and the larger bioeston fraction) and negatively correlated with water pH on the second CCA axis, which accounted for a cumulative explained variance of 74% (Fig. 13); however, the variance was not significantly explained by the Monte Carlo test ($F = 7.166, p = 0.256$ for CCA1 and $F = 1.022, p = 0.480$ for all axes). Bottom depths were discriminated by the first CCA axis, grouping shallow waters (<125 m) and deep waters (200 m). The deep waters were represented by *S. pachygaster* and the shallow waters were inhabited by the five other species. Species in shallow waters were divided into two groups. *L. suezensis* and *T. flavimaculosus*, both of which correlated with the biological parameters, and these two species contributed abundance positively to shallower waters more than the other three shallower water species (Fig. 13).

Discussion

This study shows the spatial and temporal distribution and population dynamics of six pufferfish species in the Gulf of Antalya. In general, most studies of the eastern Mediterranean Sea focus first on local records and length-weight relationships of single pufferfish species, especially *L. sceleratus* (Aydın, 2011; Özbek *et al.*, 2017). Ecological studies on fish populations in this region were recently

started by de Meo *et al.* (2018), with a focus on the spatio-temporal dynamics of the entire fish community.

Six species of pufferfish were found in the study area. The most invasive species was *L. suezensis*, with abundance up to 10,000 ind/km². Based on frequency of occurrence, two rare species, *T. spinosissimus* and *S. pachygaster*, were discovered. The other four species had moderate abundance up to 700 ind/km². Abundance of species within the genus *Lagocephalus* tended to differ among regions, with higher density in the estuarine area and in October and February. Along Egyptian coasts, these species reached maximum density between autumn and winter (El-Hawwet *et al.*, 2016). *Lagocephalus sceleratus*, which commonly occur between seafloor depths of 18 and 100 m in the Indo-Pacific (Smith & Heemstra, 1986), colonized and became established rapidly in the coastal area of the Nile Delta (Halim & Rizkalla, 2011). From there it spread towards the Algerian coast, where it was found at a depth of bottom of 50–60 m (Kara *et al.*, 2015), and towards the easternmost coast of Turkey up to the Dardanelles Strait in the Sea of Marmara (Irmak & Altınağaç, 2015; Artüz & Kubanç, 2015). The deepest location reported for *L. sceleratus* is a depth of 150 m in the Gulf of Antalya (Özbek *et al.*, 2017). In the same study, abundance was higher in winter than in summer, and it decreased along the depth gradient, following the same seasonal and spatial trends as in the present study. However, the density of *L. sceleratus* was tenfold higher than that in the present study. Moreover, *L. sceleratus* was more abundant in R2 and R3, where the bottom was covered by *Posidonia oceanica*, than in non-vegetated regions, and consistent with the results of a study by Kalogirou (2013).

In contrast to previous findings off the Lebanese coast (Boustany *et al.*, 2015), the males of *L. sceleratus* dominated over the females all year, except for February. Aydın (2011) estimated a relative abundance of 51.3% for males along the coasts of Antalya Gulf. In general, individual length, weight, and sex ratio changed with the seasons and seafloor depths. Females from the most com-

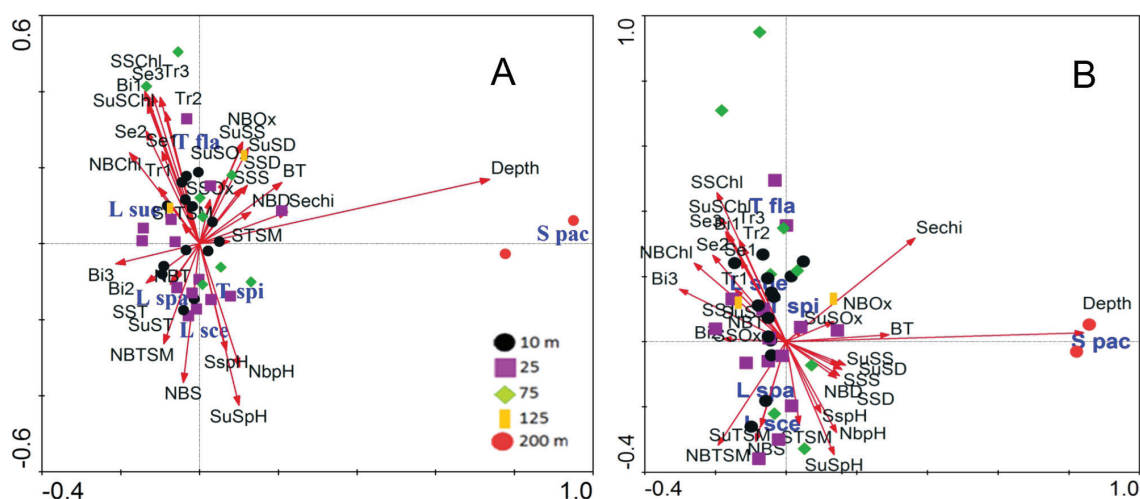


Fig. 13: CCA triplot of Tetraodontidae species (A) abundance and (B) biomass; stations classified by the bottom depths, environmental parameters (see Appendix 1 for abbreviations) and the species (*L. sce* = *Lagocephalus sceleratus*, *L. spa* = *Lagocephalus guentheri*, *L. sue* = *Lagocephalus suezensis*, *T. fla* = *Torquigener flavimaculosus*, *S. pac* = *Sphoeroides pachygaster*, and *T. spi* = *Tylerius spinosissimus*).

mon species, *L. sceleratus* were longer and heavier than males, in contrast to the findings for *L. sceleratus* along Antalya's coast (Aydın, 2011). Such sexual dimorphism in size was attributed to an increase in the fecundity of the females (Parker, 1992).

Growth was isometric for all species except *L. guentheri* and males of *L. suezensis*, which presented negative allometry. *L. suezensis* also showed negative allometric growth in a eutrophic region, the Gulf of Iskenderun, Turkey (Başusta *et al.*, 2013b). The L-W relationship of *L. sceleratus* was in line with the results of other studies in the eastern Mediterranean (Kalogirou, 2013; Boustany *et al.*, 2015; Farrag *et al.*, 2015); however, Başusta *et al.* (2013a) found *L. sceleratus* with a *b* value in Iskenderun Bay lower than our findings and the findings by Aydın (2011) in the Gulf of Antalya. Furthermore, Bilge *et al.* (2017) estimated negative allometric growths for four common pufferfish species along the coasts of Muğla, adjacent to the present study area.

T. flavimaculosus was found in high abundance in spring, but was not found in the estuarine waters; instead, it mostly inhabited the eastern part of the study area. *S. pachygaster* was the only pufferfish found at a bottom depth of 200 m; however, this species was previously caught at 80 m in the Tyrrhenian Sea (Bedini, 1998) and 180 m in the Mediterranean Sea (Tursi *et al.*, 1992; Hemida *et al.*, 2009; Farrag *et al.*, 2016; Carbonara *et al.*, 2017) and the Saroz Gulf in the Aegean Sea (Eryılmaz *et al.*, 2003), and in a range between 80 and 400 m bottom depth off the coast of Sicily (Ragonese *et al.*, 1997). Lipej *et al.* (2013) found the species at a depth of 20 m in the northernmost part of the Adriatic Sea.

The other common species (*L. guentheri*, *L. suezensis*, *L. sceleratus*) inhabited shallow waters, generally less than 75 m deep; however, *L. suezensis* was found in waters less than 40 m deep off the coasts of Syria, Israel, and Libya (Golani, 1996; Corsini *et al.*, 2005; Saad, 2005; Ben-Abdallah *et al.*, 2011), while it was caught at sites with bottom depths of 125 m in the present study. *T. spinosissimus* originated from the bathyal zone of Indo-Pacific Sea and was not observed in waters shallower than 50 m. This species spread to different parts of the Mediterranean Sea, ranging from 52 m in Iskenderun Bay, Turkey (Turan & Yaglioglu, 2011), through 50–80 m off Rhodes Island, Greece (Corsini, 2005; Corsini-Foka, 2010), down to 120 m off the coast of Tel Aviv in the eastern Mediterranean (Golani *et al.*, 2011) and below to the bathyal zone (350–400 m) off Eilat in the Red Sea (Fricke *et al.*, 2016). Abundance of all species peaked during October–February.

Each species had characteristic ranges of length and weight. The largest species (TL > 30 cm) were *L. sceleratus* and *S. pachygaster*, middle-sized species (TL 10–30 cm) were *L. guentheri*, *L. suezensis*, and *T. flavimaculosus*, and the smallest species (TL < 5 cm) was *T. spinosissimus*, which is consistent with previous reports (standard length < 3 cm, Corsini-Foka, 2010; Turan & Yaglioglu, 2011; Fricke *et al.*, 2016). *Lagocephalus sceleratus* and *L. guentheri* were reported to be larger in eutrophic Iskenderun Bay (Başusta *et al.*, 2013a) than in

the present study area and other oligotrophic regions along the Turkish coast (Taşkavak & Bilecenoğlu, 2001; Aydın, 2011). Aydın (2011) estimated six cohorts for *L. sceleratus*, which are consistent with the first four size classes of the present study. Lengths of *T. flavimaculosus* ranged from 5.5 to 13.5 cm in Rhodes Island, Greece (Corsini-Foka *et al.*, 2006). Among the common species in this study, the maximum length of *L. sceleratus* and *L. suezensis* were observed in the coldest months (October–February), whereas the total length of *L. guentheri* and *T. flavimaculosus* was higher in the warmest months (May–August). However, spatio-temporal distribution of length of *L. sceleratus* was discordant with previous results (Özbek *et al.*, 2017). At Rhodes Island, large-sized individuals of *L. sceleratus* densely populated the sandy bottom in autumn, while small-sized individuals (5–6 cm) dominated the seagrass habitat during spawning time in summer, retreating to sandy bottoms thereafter. As individuals grew in length, they performed an ontogenic migration retreating to greater depths during autumn (Kalogirou, 2013).

Sex ratios changed in both space (region and depth) and time (season). The females of *L. sceleratus* and *L. guentheri* dominated in the non-fishing zone, whereas females of *L. suezensis* were dominant in the westernmost region of the fishing zone. In general, abundance of females and males showed similar trends with respect to length over time, but decreased as bottom depth increased. Two rare species were observed only in the cold season (October–February). Females of *S. pachygaster* were longer and heavier than males, consistent with that reported along Sicilian coasts (Ragonese *et al.*, 1997).

Pufferfish were distributed primarily according to depth of seafloor. *Sphoeroides pachygaster* was discriminated far away from species that inhabit shallow waters on the CCA orientation. Most pufferfish species are of tropical origin; however, distribution did not correlate with hydrographical parameters, especially water temperature. This could be due to a change in population dynamics between seasons because small-sized individuals were observed during spawning time in spring and summer, while larger fish occurred in autumn and winter.

Densities of *L. suezensis* and *T. flavimaculosus* correlated positively with chl-*a* and seston concentrations and negatively with water pH and salinity, in contrast to the other shallow water species. However, pufferfish feed on macrobenthos and fish (Aydın, 2011; Kalogirou, 2013). Previous studies in the Gulf of Antalya showed a significant and positive correlation of the crustacean community with bioseston and chl-*a* (Patania, 2015) and of the fish assemblages in shallow waters (10–25 m) with the fine fraction comprised of seston and the near-bottom chl-*a* (de Meo *et al.*, 2018). *Torquigener flavimaculosus* was mostly found in regions near beds of *Posidonia oceanica*.

Conclusion

In conclusion, four pufferfish species have invaded and spread throughout the Gulf of Antalya in the eastern Mediterranean Sea. In addition, two invasive pufferfish species were recorded in the cold season. Spatio-temporal distribution of density, sex composition, and length-weight relationships differed remarkably among species. Species belonging to the genus *Lagocephalus* were more abundant in October–February, whereas *T. flavimaculosus* occurred mostly in spring. Regions vegetated by *Posidonia oceanica* were correlated with the density of *L. sceleratus* depending on its reproductive season.

Generally, fish weight increased isometrically with length. *Sphoeroides pachygaster* was found at bottom depths of 200 m, while the other five species inhabited shallow waters, commonly less than 75 m deep but in some cases, up to 125 m. Larger individual pufferfish appeared at deeper zones while *L. suezensis* and *T. flavimaculosus* preferred more productive regions. Abundance of other shallow water pufferfish correlated with water temperature, salinity, and pH. Estimates of population growth parameters and models of future population dynamics are recommended for further study.

Acknowledgements

The present study was funded by the Scientific Research Coordination Unit of Akdeniz University, within the framework of Project Number 2014.01.0111.001, principally coordinated by Erhan Mutlu. This study was part of Ilaria de Meo' MSc thesis and Claudia Miglietta's MSc thesis. We thank Ahmet Şahin, M. Tunca Olguner, and Cansu Olguner for their help onboard the *R/V Akdeniz Su*. We thank the two anonymous referees for their valuable comments.

References

- Akyol, O., Aydın, İ., 2016. A new record of *Lagocephalus guentheri* (Tetraodontiformes: Tetraodontidae) from the north-eastern Aegean Sea. *Zoology in Middle East*, 62 (3), 271-273.
- Akyol O., Aydın I., 2017. Occurrence of blunthead puffer, *Sphoeroides pachygaster* (Müller and Troschel, 1848) (Tetraodontidae) in north-eastern Aegean Sea (Izmir Bay, Turkey). *Journal of Applied Ichthyology*, 33, 524-526.
- Akyol, O., Unal, V., Ceyhan, T., Bilecenoglu, M., 2005. First confirmed record of *Lagocephalus sceleratus* (Gmelin, 1789) in the Mediterranean Sea. *Journal of Fish Biology*, 66, 1183-1186.
- Al-Mabruk, S.A.A., Vasilis-Orestis, S., Periklis, K., Giovos, I., 2018. The first record of *Torquigener flavimaculosus* (Tetraodontiformes: Tetraodontidae) from Libya. *International Journal of Fisheries and Aquatic Studies*, 6 (4), 449-450.
- Alshawy, F., Ibrahim, A., Hussein, C., Lahlah, M., 2019. First record of the oceanic puffer *Lagocephalus lagocephalus* (Linnaeus, 1758) from the Syrian marine waters (eastern Mediterranean). *Marine Biodiversity Records*, 12 (1), 11.
- Artüz, M. L., Kubanç, S.N., 2015. First record of the Lessepsian migrant *Lagocephalus sceleratus* (Gmelin, 1789) (Tetraodontidae) in the Sea of Marmara. *Thalassas*, 31 (2), 55-58.
- Aydın, M., 2011. Growth, Reproduction and diet of pufferfish (*Lagocephalus sceleratus* Gmelin, 1789) from Turkey's Mediterranean Sea Coast. *Turkish Journal of Fisheries and Aquatic Sciences*, 11, 569-576.
- Azzurro, E., Castriota, L., Falautano, M., Bariche, M., Broglio, E. et al., 2016. New records of the silver-cheeked toadfish *Lagocephalus sceleratus* (Gmelin, 1789) in the Tyrrhenian and Ionian Seas: early detection and participatory monitoring in practice. *BioInvasions Records*, 5 (4), 295-299.
- Başusta, A., Başusta, N., Özer, E.I., 2013a. Length-weight relationship of two puffer fishes, *Lagocephalus sceleratus* and *Lagocephalus spadiceus*, from Iskenderun Bay, northeastern Mediterranean, Turkey. *Pakistan Journal of Zoology*, 45 (4), 1047-1051.
- Başusta, A., Başusta, N., Özer, E.I., Girgin, H., Aslan, E., 2013b. Some Population Parameters of The Lessepsian Suez Puffer (*Lagocephalus suezensis*) From Iskenderun Bay, Northeastern Mediterranean, Turkey. *Pakistan Journal of Zoology*, 45 (6), 1779-1782.
- Bedini, R., 1998. First record of *Sphoeroides pachygaster* (Tetraodontidae) from the northern Tyrrhenian Sea. *Cybi-um*, 22 (1), 94-96.
- Beköz, A.B., Beköz, S., Yılmaz, E., Tüzün, S., Beköz, Ü., 2013. Consequences of the increasing prevalence of the poisonous *Lagocephalus sceleratus* in southern Turkey. *Emergency Medicine Journal*, January 2013.
- Belmaker, J., Parravicini, V., Kulbicki, M., 2013. Ecological traits and environmental affinity explain Red Sea fish introduction into the Mediterranean. *Global Change Biology*, 19, 1373-1382.
- Ben-Abdallah, A., Al-Turky, A., Nafti, A., Shakman, E., 2011. A new record of a Lessepsian fish, *Lagocephalus suezensis* (Actinopterygii: Tetraodontiformes: Tetraodontidae), in the south Mediterranean (Libyan coast). *Acta Ichthyologica Et Piscatoria*, 41 (1), 71-72.
- Bilecenoglu, M., Kaya, M., Akalin, S., 2006. Range expansion of silverstripe blaasop, *Lagocephalus sceleratus* (Gmelin, 1789), to the northern Aegean Sea. *Aquatic Invasions*, 1 (4), 289-291.
- Bilge, G., Filiz, H., Yapici, S., 2017. Length-weight relationships of four Lessepsian puffer fish species from Muğla coasts of Turkey. *Natural and Engineering Sciences*, 2 (3), 36-40.
- Boustany, L., Indary, S.E., Nader, M., 2015. Biological characteristics of the Lessepsian pufferfish *Lagocephalus sceleratus* (Gmelin, 1789) off Lebanon. *Cahiers de Biologie Marine*, 56, 137-142.
- Carbonara, P., Kolutari, J., Đurović, M., Gaudio, P., Ikica, Z. et al., 2017. The presence of Tetraodontidae species in the Central Mediterranean: an update from the southern Adriatic Sea. *Acta Adriatica*, 58 (2), 325-338.
- Çelik, M., Deidun, A., Uyan, U., Giovos, I., 2018. Filling the gap: a new record of diamondback puffer (*Lagocephalus guentheri* Miranda Riberio, 1915) from the west-eastern Mediterranean Sea, Turkey. *Journal of Black Sea/Mediterranean Environment*, 24 (2), 180-185.

- CIESM, 2020. CIESM Atlas of Exotic Fishes in the Mediterranean Sea. <http://www.ciesm.org/atlas/appendix1.html>, accessed on 27 May 2020.
- Corsini, M., Margies, P., Kondilatos, G., Economidis, P.S., 2005. Lessepsian migration in Aegean Sea: *Tylerius spinosissimus* (Pisces, Tetraodontidae) new for the Mediterranean, and six more fish records from Rhodes. *Cybium*, 29 (4), 347-354.
- Corsini-Foka, M., Margies, P., Kondilatos, G., Economidis, P.S., 2010. Tetraodontid colonizers in the Aegean Sea; Second record of the spiny blaasop, *Tylerius spinosissimus* (Actinopterygii: Tetraodontiformes: Tetraodontidae). *Acta Ichthyologica Et Piscatoria*, 40 (1), 71-74.
- Corsini-Foka, M., Margies, P., Kondilatos, G., Economidis, P., 2006. *Torquigener flavimaculosus* Hardy and Randall, 1983 (Pisces: Tetraodontidae) off Rhodes island marine area: a new alien fish in the Hellenic waters. *Mediterranean Marine Science*, 7 (2), 73-76.
- de Meo, I., Miglietta, C., Mutlu, E., Deval, M.C., Balaban, C. *et al.*, 2018. Ecological distribution of demersal fish species in space and time on the shelf of Antalya Gulf, Turkey. *Marine Biodiversity*, 48 (4), 2105-2118.
- Deidun, A., Fenech-Farrugia, A., Castriota, L., Falautano, M., Azzurro, E. *et al.*, 2015. First record of the silver-cheeked toadfish *Lagocephalus sceleratus* (Gmelin, 1789) from Malta. *BioInvasions Records*, 4 (2), 139-142.
- Dulčić, J., Dragičević, B., 2014. Occurrence of Lessepsian migrant *Lagocephalus sceleratus* (Tetraodontidae) in the Adriatic Sea. *Cybium*, 38 (3), 238-240.
- El-Haweet, A.A.K., Farrag, M.M.S., Akel, E.A., Moustafa, M.A., 2016. Puffer Fish Catch in the Egyptian Mediterranean Coast "The Challenged Invaders". *International Journal of Ecotoxicology and Ecobiology*, 1 (1), 13-19.
- Eryilmaz, L., Özulug, M., Meriç, N., 2003. The Smooth Pufferfish, *Sphoeroides pachygaster* (Müller & Troschel, 1848) (Teleostei: Tetraodontidae), new to the Northern Aegean Sea. *Zoology in the Middle East*, 28, 125-126.
- Farrag, M.M.S., El-Haweet, A.E. A.K., Akel, E.A., Moustafa, M.A., 2015. Stock status of pufferfish *Lagocephalus sceleratus* (Gmelin, 1789) along the Egyptian Coast, Eastern Mediterranean Sea. *American Journal of Life Sciences*, 3 (6-1), 83-93.
- Farrag, M.M.S., El-Haweet, A.A.K., Akel, El-S.Kh A., Moustafa, M.A., 2016. Occurrence of puffer fishes (Tetraodontidae) in the eastern Mediterranean, Egyptian coast - filling in the gap. *BioInvasions Records*, 5 (1), 47-54.
- Fricke, R., Golani, D., Appelbaum-Golani, B., Zajonz, U., 2016. New record of the spiny pufferfish, *Tylerius spinosissimus* (Regan, 1908), from Israel, Gulf of Aqaba, Red Sea (Actinopterygii: Tetraodontiformes: Tetraodontidae). *Acta Ichthyologica Et Piscatoria*, 46 (2), 115-118.
- Giordano, D., Profeta, A., Pirrera, L., Soraci, F., Perdichizzi, F., *et al.*, 2012. On the Occurrence of the blunthead Puffer, *Sphoeroides pachygaster* (Osteichthyes: Tetraodontidae), in the Strait of Messina (CentralMediterranean). *Journal of Marine Biology*, 462407, 3.
- Golani, D., 1996. The marine ichthyofauna of the eastern Levant-history, inventory and characterization. *Israel Journal of Zoology*, 42, 15-55.
- Golani, D., Sonin, O., Edelist, D., 2011. Second records of the o extension of *Tylerius spinosissimus* in the Mediterranean. *Aquatic Invasions*, 6 (1), S7-S11.
- Halim, Y., Rizkalla, S., 2011. Aliens in Egyptian Mediterranean waters. A check-list of Erythrean fish with new records. *Mediterranean Marine Science*, 12 (2), 479-490.
- Hemida, F., Ben Amor, M.M., Capapé, C., 2009. First confirmed record of the blunthead puffer, *Sphoeroides pachygaster* (Osteichthyes: Tetraodontidae) off the Algerian coast (southwestern Mediterranean). *Pan-American Journal of Aquatic Sciences - PANAMJAS*, 4 (2), 188-192.
- Irmak, E., Altınağaç, U., 2015. First record of an invasive Lessepsian migrant, *Lagocephalus sceleratus* (Actinopterygii: Tetraodontiformes: Tetraodontidae), in the Sea of Marmara. *Acta Ichthyologica Et Piscatoria*, 45 (4), 433-435.
- Kalogirou, S., Corsini-Foka, M., Sioulas, A., Wennhage, H., Pihl, L., 2010. Diversity, structure and function of fish assemblages associated with *Posidonia oceanica* beds in an area of the eastern Mediterranean Sea and the role of non-indigenous species. *Journal of Fish Biology*, 77, 2338-2357.
- Kalogirou, S., Wennhage, H., Pihl, L., 2012. Non-indigenous species in Mediterranean fish assemblages: Contrasting feeding guilds of *Posidonia oceanica* meadows and sandy habitats. *Estuarine, Coastal and Shelf Science*, 96, 209-218.
- Kalogirou, S., 2013. Ecological characteristics of the invasive pufferfish *Lagocephalus sceleratus* (Gmelin, 1789) in the eastern Mediterranean Sea - a case study from Rhodes. *Mediterranean Marine Science*, 14 (2), 251-260.
- Kan, S., Chan, M.K., David, P., 1987. Nine fatal cases of puffer fish poisoning in Sabah, Malaysia. *Medical Journal of Malaysia*, 42, 199-200.
- Kara, M.H., Ben Lamine, E., Francour, P., 2015. Range expansion of an invasive pufferfish, *Lagocephalus sceleratus* (Actinopterygii: Tetraodontiformes: Tetraodontidae), to the south-western Mediterranean. *Acta Ichthyologica Et Piscatoria*, 45 (1), 103-108.
- Kideys, A.E., 2002. Fall and rise of the Black Sea ecosystem. *Science*, 297 (5586), 1482-1484.
- Kiparissis, S., Peristeraki, P., Tampakakis, K., Kosoglou, I., Doudoumis, V. *et al.*, 2018. Range expansion of a restricted lessepsian: westbound expansion breakthrough of *Lagocephalus spadiceus* (Richardson, 1844) (Actinopterygii: Tetraodontidae). *BioInvasions Records*, 7 (2), 197-203.
- Kleitou, P., Giovos, I., Tiralongo, F., Doumpas, N., Bernardi, G., 2019. Westernmost record of the diamondback puffer, *Lagocephalus guentheri* (Tetraodontiformes: Tetraodontidae) in the Mediterranean Sea: First record from Greek waters. *Journal of Applied Ichthyology*, 35, 576-579.
- Koç, H.T., Erdoğan, Z., Üstün F., 2011. Occurrence of the Lessepsian migrant, *Lagocephalus sceleratus* (Gmelin 1789) (Osteichthyes: Tetraodontidae), in Iskenderun Bay (north-eastern Mediterranean, Turkey). *Journal of Applied Ichthyology*, 27, 148-149.
- Lipej, L., Mavrič, B., Paliska, D., 2013. New northernmost record of the blunthead pufferfish, *Sphoeroides pachygaster* (Osteichthyes: Tetraodontidae) in the Mediterranean Sea. *Annales, Series Historia Naturalis*, 23, 103-114.
- Lorenzen, C.J., 1967. Determination of chlorophyll and phaeopigments: spectrophotometric equations. *Limnology and Oceanography*, 12, 343-346.

- Matsuura, K., Golani D., Bogorodsky S.V., 2011. The first record of *Lagocephalus guentheri* Miranda Ribeiro, 1915 from the Red Sea with notes on previous records of *L. lunaris* (Actinopterygii, Tetraodontiformes, Tetraodontidae). *Bulletin of the National Museum of Nature and Science. Series A, Zoology*, 37 (3), 163-169.
- Mutlu, E., Balaban, C., 2018. New algorithms for the acoustic biomass estimation of *Posidonia oceanica*: a study in the Antalya Gulf (Turkey). *Fresenius Environmental Bulletin*, 27 (4), 2555-2561.
- Nader, M.R., Indary, S., Boustany, L.E., 2012. The puffer fish *Lagocephalus sceleratus* (Gmelin, 1789) in the eastern Mediterranean. EastMed Technical Document No. 10. GCP/INT/041/EC-GRE-ITA/TD-10. EstMed FAO, Athens, Greece.
- Öndes, F., Ünal, V., Özbilgin, H., Deval, C., Turan, C., 2018. By-catch and monetary loss of pufferfish in Turkey, the Eastern Mediterranean. *Ege Journal of Fisheries and Aquatic Sciences*, 35 (4), 361-372.
- Özbek, E.Ö., Çardak, M., Kebapçioğlu, T., 2017. Spatio-temporal patterns of abundance, biomass and length of the silver-cheeked toadfish *Lagocephalus sceleratus* in the Gulf of Antalya, Turkey (eastern Mediterranean Sea). *Turkish Journal of Fisheries and Aquatic Sciences*, 17, 725-733.
- Parker, G.A., 1992. The evolution of sexual size dimorphism in fish. *Journal of Fish Biology*, 41, 1-20.
- Patania, A., 2015. Megistobenthic faunal diversity of Antalya Gulf: Crustacea. Università Degli Studi di Bologna Scuola Di Scienze Corso Di Laurea Magistrale in Biologia Marina, Italy, MSc Thesis, October, 2015.
- Patmavathi, P., Sujatha, K., Deepti, V.A.I., 2017. Studies on length groups and length-weight relationship of puffer fishes (Pisces: Tetraodontidae) in the catches off Visakhapatnam, India. *Indian Journal of Geo Marine Sciences*, 46 (5), 972-981.
- Pauly, D., 1980. On the interactions between natural mortality, growth parameters and mean environmental temperature in 175 fish stocks. *Conseil Permanent International pour l'Exploration de la Mer*, 39 (3), 175-192.
- Ragonese, S.; Jereb, P.; Morara, U., 1997. Morphometric relationships of *Sphoeroides pachygaster* (Pisces - Tetraodontidae) of the Strait of Sicily (Mediterranean Sea). *Cahiers de Biologie Marine*, 38 (4), 283-289.
- Reina-Hervas, J.A., Raso, O.J.E.G., Manjon-Cabeza, M.E., 2004. First record of *Sphoeroides spengleri* (Osteichthyes: Tetraodontidae) in the Mediterranean Sea. *Journal of the Marine Biological Association of the United Kingdom*, 84, 1089-1090.
- Saad, A., 2005. Check-list of bony fish collected from the coast of Syria. *Turkish Journal of Fisheries and Aquatic Sciences*, 5, 99-106.
- Santhanam, R., 2018. Biology and ecology of toxic Pufferfish, USA. In: Taylor & Francis group.
- Saville, A., 1977. Survey methods of appraising fisheries resources. FAO Fisheries Technical Paper, 171, 76 p.
- Shimazaki, H., Shinomoto, S., 2007. A method for selecting the bin size of a time histogram. *Neural Computation*, 19, 1503-1527.
- Simon, K.D., Mazlan, A.G., 2008. Length-weight and length-length relationships of Archer and Puffer fish species. *The Open Fish Science Journal*, 1, 19-22.
- Smith, M.M., Heemstra, P.C., 1986. Smith's Sea Fishes. Smith Institute of Ichthyology Press, Grahamstown, Republic of South Africa.
- Streftaris, N., Zenetos, A., 2006. Alien marine species in the Mediterranean - the 100 'worst invasives' and their impact. *Mediterranean Marine Science*, 7 (1), 87-118.
- Tamele, I., Silva, M., Vasconcelos, V., 2019. The incidence of tetrodotoxin and its analogs in the Indian Ocean and the Red Sea. *Marine Drugs*, 17 (1), 28.
- Taşkavak, E., Bilecenoglu, M., 2001. Length-weight relationships for 18 Lessepsian (Red Sea) immigrant fish species from the eastern Mediterranean coast of Turkey. *Journal of the Marine Biological Association of the United Kingdom*, 81, 895-896.
- Tuncer, S., Aslan-Cihangir, H., Bilecenoglu, M., 2008. First record of the Lessepsian migrant *Lagocephalus spadiceus* (Tetraodontidae) in the Sea of Marmara. *Cybium*, 32 (4), 347-348.
- Turan, C., Yaglioglu, D., 2011. First record of the Spiny blaasop *Tylerius spinosissimus* (Regan, 1908) (Tetraodontidae) from the Turkish coasts. *Mediterranean Marine Science*, 12 (1), 247-252.
- Turan, C., Gürlek, M., Ergüden, D., Uyan, A., Karan, S. et al., 2017. Assessing DNA Barcodes for Identification of Pufferfish Species (Tetraodontidae) in Turkish Marine Waters. *Natural and Engineering Sciences*, 2 (3), 55-66.
- Tursi, A., Donghia, G., Matarrese, A., 1992. First finding of *Sphoeroides pachygaster* (Muller & Troschel, 1848) (Tetraodontidae) in the Ionian Sea (Middle Eastern Mediterranean). *Cybium*, 16 (2), 171-172.
- Ünal, V., Göncüoğlu, H., Durgun, D., Tosunoğlu, Z., Deval, M.C. et al., 2015. Silver-cheeked toadfish, *Lagocephalus sceleratus* (Actinopterygii: Tetraodontiformes: Tetraodontidae), causes a substantial economic losses in the Turkish Mediterranean coast: A call for decision Makers. *Acta Ichthyologica Et Piscatoria*, 45 (3), 231-237.
- Yang, C.C., Liao, S.C., Deng, J.F., 1996. Tetrodotoxin poisoning in Taiwan; an analysis of poison center data. *Veterinary and Human Toxicology*, 38, 282-286.

Appendix

Appendix 1. Environmental parameters with abbreviations used in statistical analyses (prefixes for abbreviations: SS = sea surface, Su = sub-surface, and NB = near-bottom water).

Physicochemical parameters	Biological parameters
Secchi disk depth (m); Secchi	Seston - 1 mm (g/m ³); Se1
Oxygen (mg/l); Ox	Seston - 0,5 mm (g/m ³); S2
Temperature (°C); T	Seston - 0,063 mm (g/m ³); S3
Salinity (PSU); S	Bioseston - 1 mm (g/m ³); Bi1
pH; pH	Bioseston - 0,5 mm (g/m ³); Bi2
Density, σ_t ; D	Bioseston - 0,063 mm (g/m ³); Bi3
Total Suspended Matter (mg/l); TSM	Tripton - 1mm (g/m ³); Tr1
Chl- <i>a</i> (mg/l); Chl	Tripton - 0,5mm (g/m ³); Tr2
Bottom types; BT (de Meo <i>et al.</i> , 2018)	Tripton - 0,063mm (g/m ³); Tr3